Omodeo-Salé, S., Ondrak, R., Arribas, J., Mas, R., Guimerà, J., Martínez, L. (2019): Petroleum Systems Modelling in a Fold-and-Thrust Belt Setting- The Inverted Cameros Basin, North-Central Spain. - *Journal of Petroleum Geology*, *42*, 2, pp. 145—171.

DOI: http://doi.org/10.1111/jpg.12728

JPG Journal of Petroleum Geology www.jpg.co.uk

PETROLEUM SYSTEMS MODELLING IN A FOLD-AND-THRUST BELT SETTING: THE INVERTED CAMEROS BASIN, NORTH-CENTRAL SPAIN

S. Omodeo-Salé[1+*], R. Ondrak[2], J. Arribas[1], R. Mas[3], J. Guimerà[4] and L. Martínez[5]

The Mesozoic Cameros Basin, northern Spain, was inverted during the Cenozoic Alpine orogeny when the Tithonian – Upper Cretaceous sedimentary fill was uplifted and partially eroded. Tar sandstones outcropping in the southern part of the basin and pyrobitumen particles trapped in potential source rocks suggest that hydrocarbons have been generated in the basin and subsequently migrated. However, no economic accumulations of oil or gas have yet been found. This study reconstructs the evolution of possible petroleum systems in the basin from initial extension through to the inversion phase, and is based on structural, stratigraphic and sedimentological data integrated with petrographic and geochemical observations. Petroleum systems modelling was used to investigate the timing of source rock maturation and hydrocarbon generation, and to reconstruct possible hydrocarbon migration pathways and accumulations.

In the northern part of the basin, modelling results indicate that the generation of hydrocarbons began in the Early Berriasian and reached a peak in the Late Barremian – Early Albian. The absence of traps during peak generation prevented the formation of significant hydrocarbon accumulations. Some accumulations formed after the deposition of post-extensional units (Late Cretaceous in age) which acted as seals. However, during subsequent inversion, these reservoir units were uplifted and eroded.

In the southern sector of the basin, hydrocarbon generation did not begin until the Late Cretaceous due to the lower rates of subsidence and burial, and migration and accumulation may have taken place until the initial phases of inversion. Sandstones impregnated with bitumen (tar sandstones) observed at the present day in the crests of surface anticlines in the south of the basin are interpreted to represent the relics of these palaeo-accumulations.

Despite a number of uncertainties which are inherent to modelling the petroleum systems evolution of an inverted and overmature basin, this study demonstrates the importance of integrating multidisciplinary and multi-scale data to the resource assessment of a complex fold-and-thrust belt.

[1] Departamento de Mineralogía y Petrología, UCM, IGEO (UCM-CSIC), Madrid, Spain.
[2] Section Organic Geochemistry, GFZ, German Research Centre for Geosciences, Potsdam, Germany.
[3] Departamento de Geodinámica, Estratigrafía y Paleontología, UCM, IGEO (UCM-CSIC), Madrid, Spain.
[4] Dept. de Dinàmica de la Terra i de l'Oceà, Facultat de Ciències de la Terra, Universitat de Barcelona, Spain.
[+]Corresponding author, Silvia.OmodeoSale@unige.ch

Key words: petroleum systems modelling, fold-and-thrust belt, basin inversion, source rock, migration, tar sandstones, palaeo reservoirs, Cameros Basin, Cretaceous, Spain.

[5] EOST, Université de Strasbourg, Strasbourg, France.
* *Current address:* Department of Earth Science, University of Geneva, Switzerland.

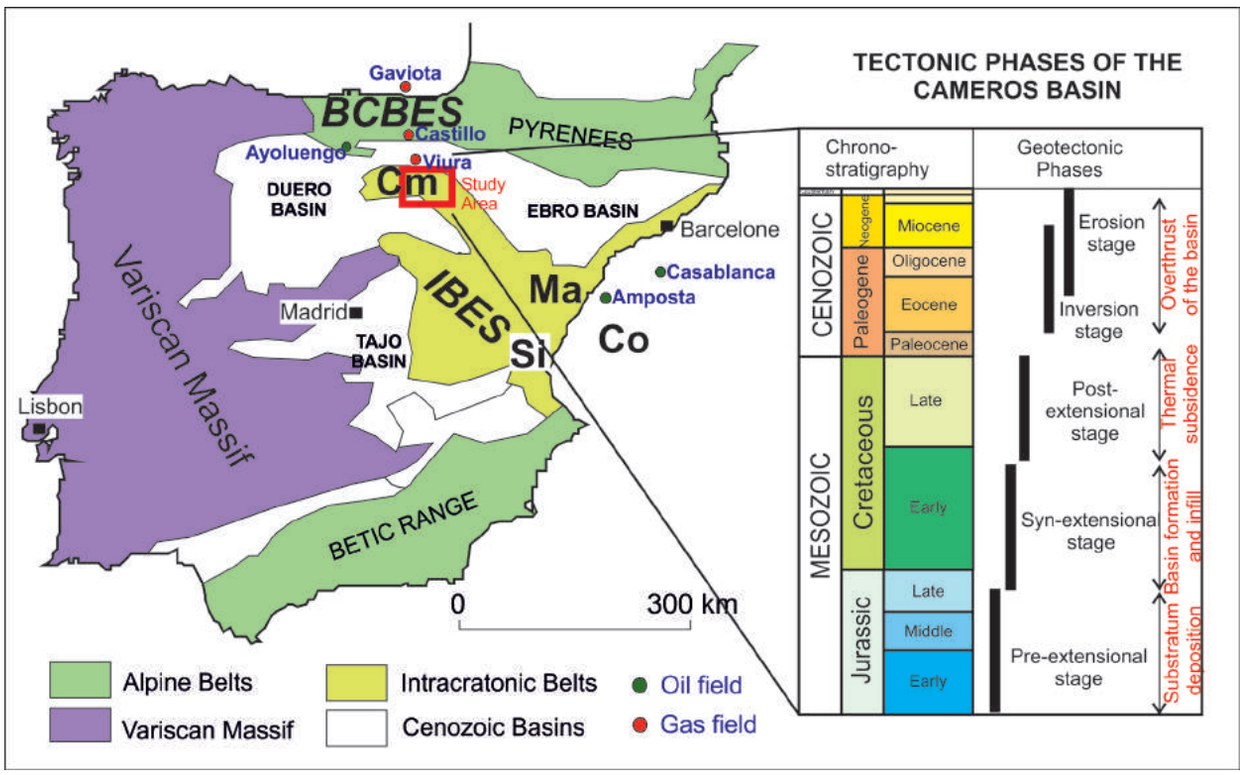

Fig. 1. Outline map of the Iberian peninsula showing the extent of the Mesozoic Iberian Extensional System (IBES) which includes the Cameros Basin (Cm), the focus of this study (modified from Mas *et al.*, 2004). The chart at right shows the tectonic phases associated with formation, extension and inversion of the Cameros Basin. BCBES, Basque – Cantabrian Extensional System; Ma, Maestrat Basin; Si, South Iberian Basin; Co, Columbrets Basin.

INTRODUCTION

Extensional basins are favorable settings for the formation of commercial hydrocarbon reserves (Magoon and Dow, 1994; Mann *et al.*, 2003; Davison and Underhill, 2012; Allen and Allen, 2017). However, a precise relative timing of depositional, tectonic and thermal events is necessary in order to generate and trap commercial volumes of hydrocarbons. This is particularly challenging in extensional basins that have subsequently been inverted and stacked in a thrust belt. In such complex settings, the timing of hydrocarbon expulsion from the source rocks with respect to the timing of inversion-related folding and faulting is crucial. If expulsion and migration occurred before inversion, potential accumulations may be destroyed; however if the source rocks generated hydrocarbons during or after inversion, hydrocarbons may accumulate in developing structural traps.

Petroleum systems modelling is routinely used to determine whether the many factors required for hydrocarbon generation and accumulation are present and fit together in time and space. Modelling allows an evaluation to be made of the factors controlling the timing of hydrocarbon generation and accumulation, and to estimate the potential volumes of hydrocarbon resources (e.g. Welte *et al.*, 1997). In inverted basins, modelling can be challenging as the basin infill has been deformed and partially eroded, resulting in uncertainties in the initial basin geometry. Structural restoration is therefore required. Furthermore, horizontal and vertical deformation through time is difficult to reproduce in modelling software, although recently-developed tools allow tectonics and thrusting to be better integrated into the petroleum systems simulation (IES, 2007; Callies *et al.*, 2018).

In this paper, the inverted Mesozoic Cameros Basin in the Iberian fold-and-thrust belt, north-central Spain (Fig. 1), is investigated as a modelling case study. In this general area, a number of small-scale oilfields located both on- and offshore have been discovered and have in some cases been developed. These include the Lora-Ayoluengo oilfield where production began in 1961; the Casablanca field (1982), and the Viura gasfield, where production began in 2014 (CORES, 2015a, b; Martínez del Olmo and Mallo García, 2002; Mas *et al.*, 2002, 2003; Proyecto Viura, 2014; Quesada *et al.*, 1997; Secretaría de Estado de Energía, 2014). Jurassic and Early Cretaceous source rocks charging these fields were deposited during times of global anoxia which favoured the sedimentation and preservation of organic matter (Klemme and Ulmishek, 1991). However compared to coeval Mesozoic basins elsewhere in Europe (e.g. the Paris Basin, Aquitanian

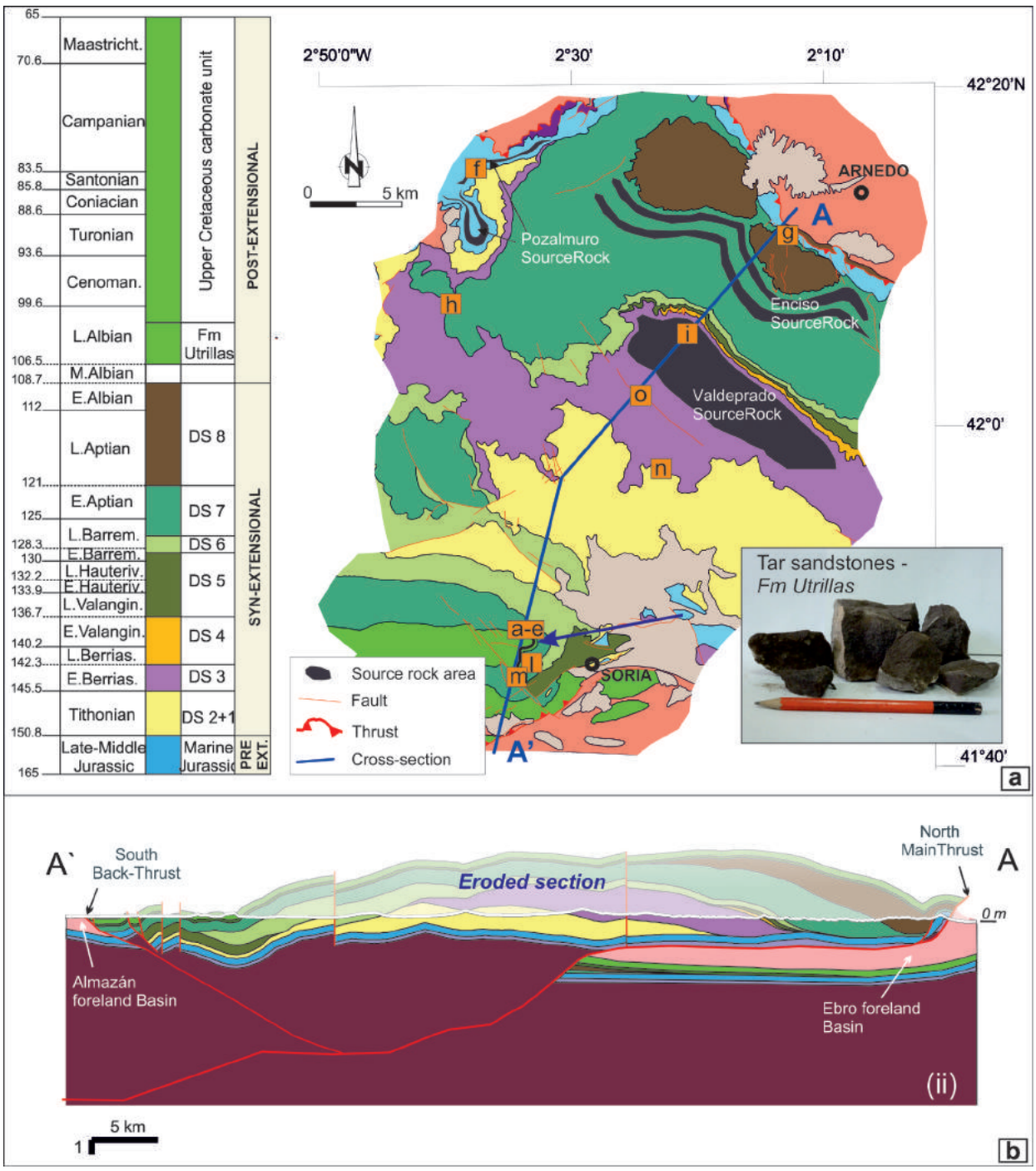

Fig. 2. (a) Surface geological map of the Cameros Basin showing the locations of potential palaeo source and reservoir rocks. The orange boxes show the location of the samples illustrated in Fig. 4.
(b) SW-NE balanced geological cross-section through the present-day inverted Cameros Basin; line of section in Fig. 2a. Map and section modified from Omodeo-Salé *et al.* (2014).

Basin and Austrian Molasse Basin), the hydrocarbon resource of the Iberian basin system is economically insignificant although high-quality source rocks are known to be present.

Reasons for the absence of commercial oil and gas accumulations in the Iberian extensional system are investigated in this study of the Cameros Basin. This inverted and partially eroded basin which developed between the Late Jurassic and Early Cretaceous was deformed and uplifted during Alpine compression (Figs 1, 2). There are multiple indications that hydrocarbons were generated, migrated and potentially accumulated in the basin. For example, bituminous sandstones are observed at outcrop along the crests of surface anticlines in the south of the basin (Fig. 2a). The bitumen was exploited in the second half of the 19th century to produce asphalt (Palacios, 1890; Puche, 2015). However no oil or gas accumulations of

economic size have so far been discovered in the basin. The traces of hydrocarbons observed in the matrix of various stratigraphic units are interpreted as the relics of hydrocarbon generation and migration processes in palaeo-source rocks and/or carrier units (Arribas *et al.*, 2014; Mantilla-Figueroa *et al.*, 1998; Ochoa *et al.*, 2007; Omodeo-Salé *et al.*, 2016). Although the evidence suggests the existence of an active petroleum system in the Cameros Basin, the origin of these hydrocarbons has been poorly investigated to-date.

A number of multidisciplinary studies have been performed in the Cameros Basin over recent decades and have investigated its tectonic and sedimentary evolution (e.g. Tischer, 1965, 1966; Beuther, 1966; Salomon, 1982a, b, 1983; Mas *et al.*, 1993; Guimerà *et al.*, 1995; Mata *et al.*, 2001; Arribas *et al.*, 2003; Benito and Mas, 2006; Casas *et al.*, 2009; Quijada *et al.*, 2013; Suárez-González *et al.*, 2013; Omodeo-Salé *et al.*, 2014; Quijada *et al.* 2016; Suarez-Gonzalez *et al.*, 2015; Mas *et al.*, 2018). The studies were in general based on outcrop data as little geophysical or subsurface data (seismic, gravimetry, wells-logs or cores) are available. Recent studies of the thermal evolution of the basin and of organic-rich intervals have improved the general understanding of the basin's burial and maturation history (Omodeo-Salé *et al.*, 2016, 2017). By integrating these multidisciplinary data, the present study attempts to reconstruct the petroleum generation, migration and accumulation history of the Cameros Basin. A 2D petroleum systems model was constructed in order (i) to investigate whether suitable conditions existed to generate economically significant volumes of hydrocarbons; (ii) to identify the main source rocks; (iii) to define the critical moments in the evolution of the petroleum system; and (iv) to consider why no oil and gas accumulations occur in the basin at the present day.

GEOLOGICAL FRAMEWORK

The inverted Cameros Basin (north-central Spain) is located in the NW of an intraplate compressional belt extending over the eastern, central and northern parts of the Iberian Peninsula (Fig. 1). Evolution of the Cameros Basin can be divided into four phases (Fig. 1): (i) a pre-extensional stage (Middle–Late Jurassic), when the substratum of the basin formed (Mas *et al.*, 1993; Salas *et al.*, 2001); (ii) an extensional stage (Tithonian to Early Albian) associated with the opening of the Western Tethys and North Atlantic (Arche and López-Gómez, 1996; Mas *et al.*, 2003; Vera, 2001; Verges and Garcia-Senz, 2001), which resulted in the deposition of the basin sedimentary infill (Salas *et al.*, 2001); (iii) a post-extensional phase (Late Albian to end-Cretaceous), when the entire basin system subsided due to thermal relaxation of the lithosphere, with the deposition of a sedimentary succession of relatively uniform thickness and facies (Alonso and Mas, 1993; García and Mas, 2004); and (iv) an inversion and erosional phase (Eocene to Early Miocene) (Casas and Salas, 1992; Salas and Casas, 1993; Salas *et al.*, 2001). During the inversion phase, a thrust sheet including the Cameros Basin was displaced by some 28 km northwards on the Northern Main Thrust onto the Ebro Foreland basin succession, and 5 km southward by a back thrust onto the Alamázan Basin foreland (Guimerà *et al.*, 1995) (Fig. 2b).

In the central-northern sector of the basin, part of the infill was affected by two low- to very low-grade hydrothermal events (Alonso-Azcárate *et al.*, 1999; Alonso-Azcárate *et al.*, 1995; Barrenechea *et al.*, 1995, 2001; Casas *et al.*, 2012; Casquet *et al.*, 1992; Del Río *et al.*, 2009; González-Acebrón *et al.*, 2011, 2012; Mantilla-Figueroa *et al.*, 1998; Mantilla-Figueroa, 1999; Mas *et al.*, 2003; Mata *et al.*, 2001; Ochoa *et al.*, 2007). The first event took place during the Late Albian to Coniacian with temperatures exceeding 350°C (Casquet *et al.*, 1992; González-Acebrón *et al.*, 2011). The second event occurred during Eocene inversion, with maximum temperatures of 280–305°C (González-Acebrón *et al.*, 2011).

Basin infill and stratigraphy

The Cameros Basin thrust sheet unit comprises the Tithonian – Upper Cretaceous syn- and post-extensional basin infill and its Jurassic and Triassic substratum together with Variscan basement (Fig. 2). The substratum of the basin formed during the pre-extensional phase and is composed of Jurassic rocks (up to Kimmeridgian in age) largely consisting of marine carbonates and shales (Alonso and Mas, 1990; Aurell and Melendez, 1993; Leinfelder, 1994; Bádenas and Aurell, 2001; Benito *et al.*, 2006) (Table 1, Fig. 3). These rocks are exposed at the surface along the northern margin of the basin and parts of the southern margin in contact with the main thrust (Fig. 2a). Geophysical data demonstrate that the substratum is present throughout the basin (Guimerà *et al.*, 1995; Mas *et al.*, 1993; Omodeo Salé *et al.*, 2014) with an estimated thickness of ca. 500 m (Fig. 2b).

The basin infill is composed of syn-extensional deposits which are Tithonian to early Albian in age (Mas *et al.*, 1993; Salas *et al.*, 2001) (Figs 2 and 3) and which are mainly composed of fluvial, lacustrine and tide-influenced sediments (Quijada *et al.*, 2013a, b; Suárez-Gonzalez *et al.*, 2013) (Table 1). The succession is up to 6500 m thick (Omodeo-Salé *et al.*, 2014; Quijada *et al*. 2016; Suarez-Gonzalez *et al.*, 2015;Mas *et al.*, 2018) and has been divided into eight depositional sequences, DS1 to DS8 (Table 1) composed of distinct lithostratigraphic units (groups and formations) (Tischer, 1965, 1966; Beuther, 1966;

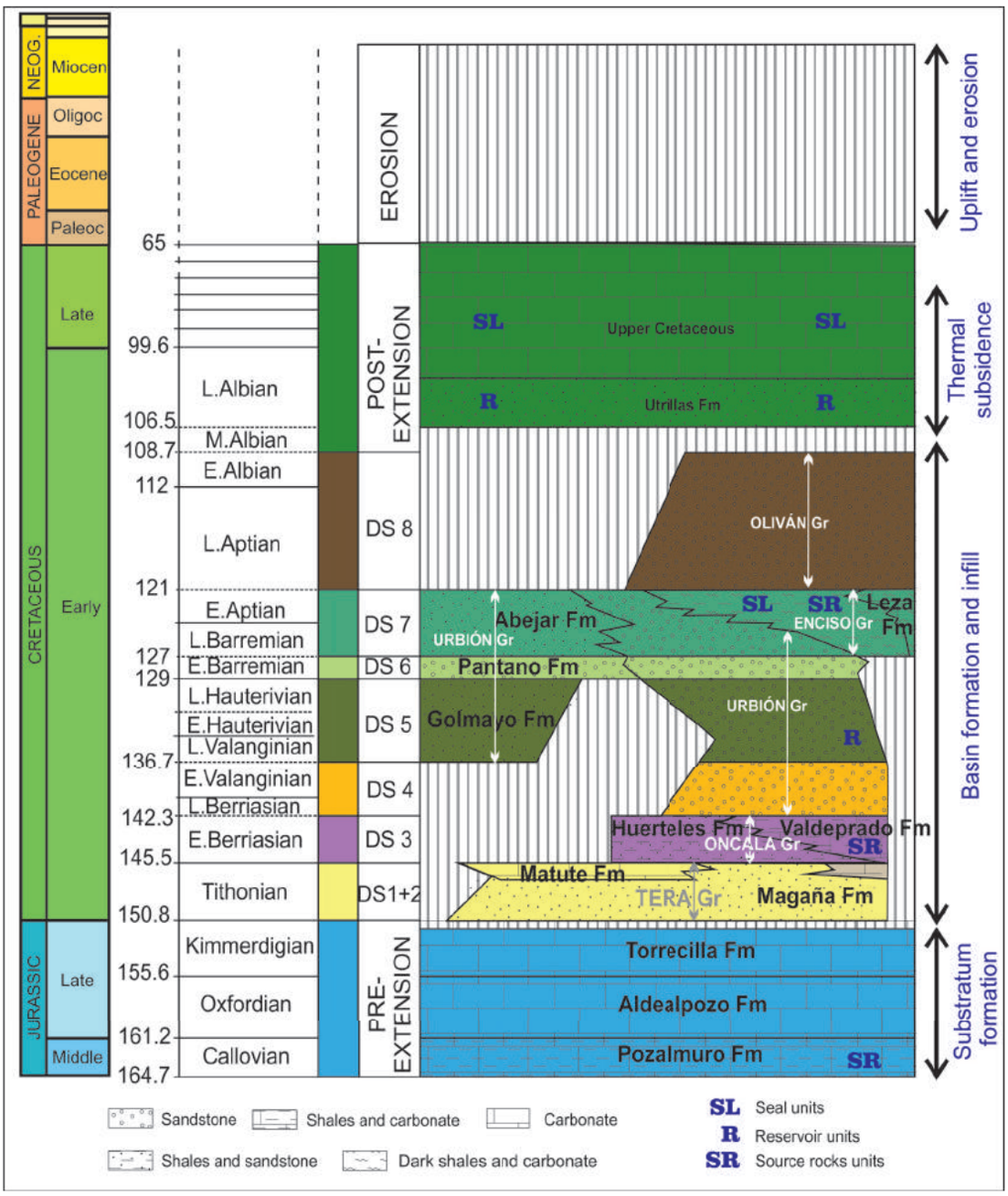

Fig. 3. Stratigraphic chart for the Cameros Basin showing the formations and groups which make up the pre-, syn- and post-extensional successions. Potential source rocks are indicated. Modified from Mas et *al.* (2011).

Salomon, 1982a, b, 1983; Mas *et al.*, 1993, 2003; Martín-Closas and Alonso-Millán, 1998; Arribas *et al.*, 2003; Quijada *et al.*, 2013a, b; Suárez-González *et al.*, 2010, 2013).

The unconformably overlying post-extensional succession (Upper Albian to Upper Cretaceous) is partially preserved only in the southern sector of the basin. An original thickness of 650 m has been estimated from interpretations of well and regional outcrop data (Mas *et al.*, 1993; Salas *et al.*, 2001; Omodeo-Salé *et al.*, 2014) (Fig. 2). In this work, this interval is divided into the Utrillas Formation sandstones and an overlying Upper Cretaceous unit which is mostly composed of limestones (Fig. 3).

PETROLEUM SYSTEM

Evidence of hydrocarbon generation, migration and accumulation in the Cameros Basin

Relic hydrocarbons in the Cameros Basin include the Utrillas Formation tar sandstones which are exposed in an anticline in the southern sector of the basin near the village of Fuentetoba (Fig. 2a; Fig. 4a-e). Due to their strongly biodegraded condition, the origin of these hydrocarbons is poorly understood (Mas *et al.*, 2003; Permanyer *et al.*, 2011).

Petrographic observations document evidence for hydrocarbon generation and expulsion in the Cameros Basin from shaley, organic-rich source rocks. In the

Table 1. Ages, lithologies and sedimentological features of the groups and formations which form the basin infill.

Age (Ma) From	Age (Ma) To	Unit	Group/Formation	Lithology	Depositional System
65.5	98	Post-rift	Upper Cretaceous	Limestone	Inner-outer marine platforms
106	108.7		Utrillas Fm	Sandstones, clay rich	Fluvial
121	108.7	DS8	Olivan Gr	Sandstone bodies interbedded with shales and minor limestone beds	Fluvial tide-influenced
127	121	DS7	Leza Fm	Micritic limestone	Coastal wetlands
			Urbión Gr	Coarse grained sandstones and shales	Fluvial, meandering
			Enciso Gr	Limestones alternating with sandstones and shales	Fluvial, coastal wetland and lagoonal
			Abejar Fm	Conglomerates and sandstone interbedded with shales	Fluvial-lacustrine
129	127	DS6	Urbión Gr	Coarse grained sandstones and shales	Fluvial, meandering
			Pantano Fm	Sandstones interbedded with conglomerates and shales	Alluvial-fluvial braided
136.7	129	DS5	Urbión Gr	Coarse grained sandstones and shales	Fluvial, meandering
			Golmayo Fm	Sandstones interbedded with shales and limestones	Fluvial-lacustrine
142.3	136.7	DS4	Urbión Gr	Coarse grained sandstones and shales	Fluvial, meandering
145.5	142.3	DS3	Valdeprado Fm	Carbonates-marls with interbedded gypsum	Shallow, perennial coastal lakes
			Huerteles Fm	Fine-grained sandstones interbedded with shales and marls	Fluvial, tide-influenced
150.8	145.5	DS1+2	Matute Fm	Micritic limestones	Lacustrine
			Magaña Fm	Conglomerates and sandstone intercalated with shales	Fluvial-alluvial
150.8	155.6	Jurassic	Torrecilla Fm	Reefal and oolitic limestones	Shallow carbonate ramp
161.2	155.6	Jurassic	Aldealpozo Fm	Limestones	Shallow carbonate ramp
164.7	161.2	Jurassic	Pozalmuro Fm	Carbonate-marls and shales	Outer platform

northern sector of the basin, particles of pyrobitumen have been found in the matrix of the shales in the Pozalmuro Formation (which constitutes the Jurassic substratum), the Valdeprado Formation (sequence DS3) and the Enciso Group (DS7) (Fig. 3). The pyrobitumen consists of dispersed, isolated particles and/or as coatings on mineral grains (Fig. 4f, g, h: see locations in Fig. 2a), and has been interpreted as a hydrocarbon residue remaining after primary cracking of kerogen (c.f. Teichmüller, 1973, 1974; Taylor *et al.*, 1998; Suárez-Ruiz *et al.*, 2012) and/or migration. The observation of a fine-grained residue in the Valdeprado Formation (DS3) (Fig. 4i) is intepreted as evidence for the thermal transformation of liptinite-rich organic matter into hydrocarbons (Omodeo-Salé *et al.*, 2016; Omodeo-Salé and Suárez-Ruiz, 2017). Thus, these units could include the original source rocks. In these deposits, pyrobitumen constitutes most of the residual organic carbon forming the TOC measured by Rock-Eval analysis in a recent study (Omodeo-Salé *et al.*, 2016) (Fig. 5a). In the DS7 and DS3 units, thermal alteration textures (coke, mesophases) were observed in the pyrobitumen particles, indicating the occurrence of secondary cracking of oil to gas (Fig. 4g, h) at temperatures over 300°C (Rahimi *et al.*, 1998; Taylor *et al.*, 1998). This was most likely related to the circulation of hydrothermal fluids (Omodeo-Salé *et al.*, 2016).

In the southern sector of the basin, in the early mature shales in the Abejar Formation (DS7 unit, Barremian), green-yellow fluorescent hydrocarbon droplets (exsudatinite), associated with hydrogenated organic matter (liptinite macerals) (Fig. 4l), have been observed, suggesting that recent hydrocarbon generation has occurred in these rocks (c.f. Teichmüller, 1973, 1974). In the same shales, high-reflectance solid

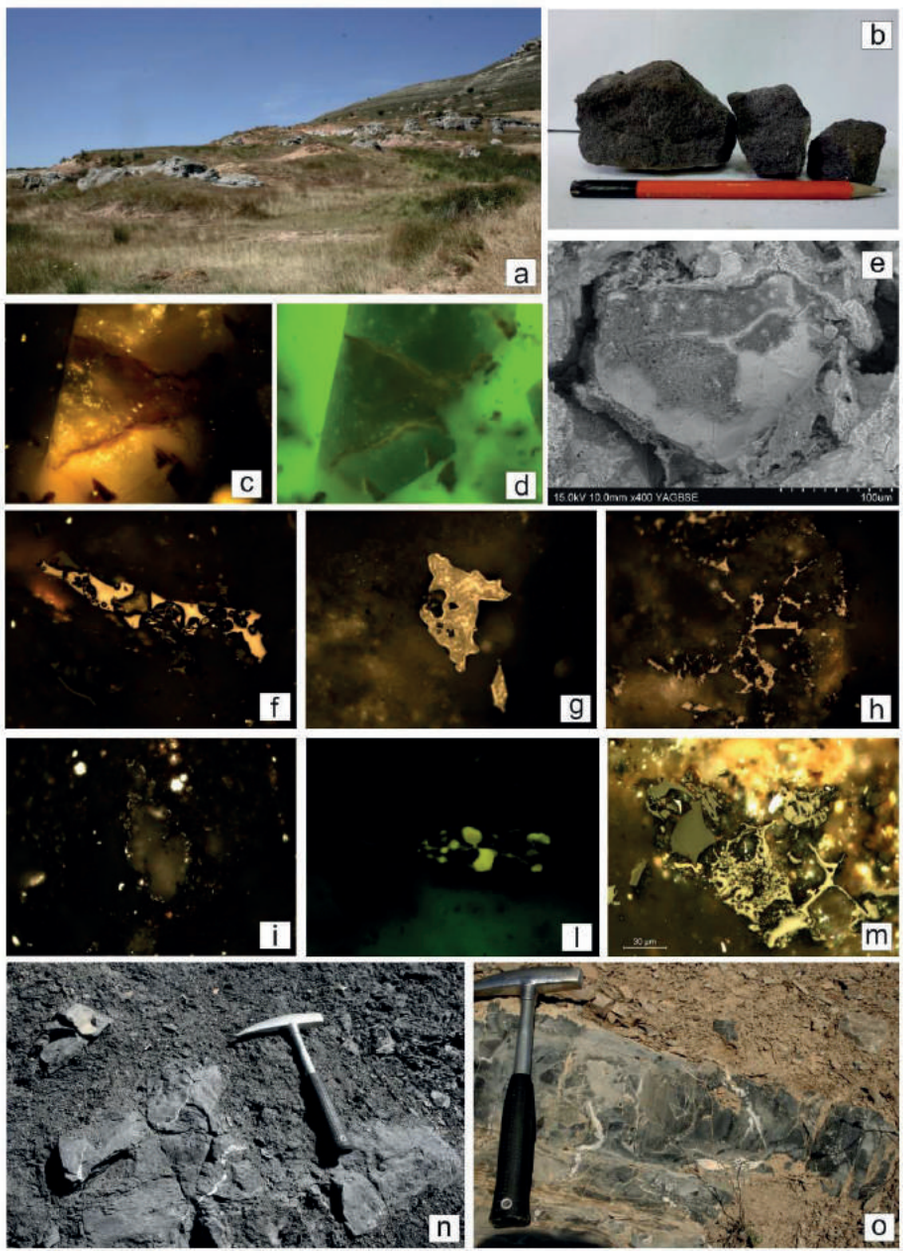

Fig. 4. Photo-plates illustrating hydrocarbon shows and traces recorded in outcrop samples from locations in the Cameros Basin (sample locations in Fig. 2a). Optical microscope observations in c, d, f, g, h, i, l and m are under reflect white light; fluorescence mode in d and l; SEM observation in e. Optical microscope photo-plates are 200 µm across.
(a) Outcrop photograph of the Utrillas Formation bituminous sandstones in the south of the Cameros Basin;
(b) hand specimens of the Utrillas Formation bituminous sandstone;
(c) Dark-brown hydrocarbons filling fractures and veins in the Utrillas Formation sandstones.
(d) as (c) in fluorescence mode illumination;
(e) SEM photomicrograph showing bitumen coating on quartz grain in the Utrillas Formation;
(f) Pyrobitumen particles in the mineral matrix of the Jurassic Pozalmuro Formation with degassing vacuoles;
(g) Pyrobitumen with thermal alteration texture indicating liquid to gas phase transition (mesophase) (DS7 unit, Leza Formation);
(h) Pyrobitumen particles with coke-like thermal alteration texture (DS3, Huerteles Formation);
(i) Fine-grained residue (micrinite) left as a result of the thermal transformation of hydrogenated organic matter (liptinite group macerals) (DS3 unit, Valdeprado Formation).
(l) Green to yellow fluorescent hydrocarbons droplets (exsudatinite), formed as a result of the thermal transformation of liptinite (DS7 unit, Abejar Formation) (fluorescence mode illumination).
(m) High-reflectance solid bitumen surrounding the margins of minerals together with immature organic matter particles (DS7 unit, Abejar Formation).
(n) and (o) Irregular fractures in units DS3 and DS1+2 in the central Cameros Basin, resulting from the migration of hydrocarbons from organic-rich source rocks, and now filled by calcite.

bitumen particles were also found (Fig. 4m). The overmature state of the bitumen with respect to the early-mature state of the host rocks suggest that it is derived from oil which has migrated from deeper-lying source rocks.

Hydrocarbon streaks between quartz grains have been observed occasionally in sandstones of the syn-extensional Urbión Group (DS4, DS5 DS6, and DS7 units) in outcrops in the central-northern part of the basin (Mantilla-Figueroa *et al.*, 1998; Mas *et al.*, 2003; Ochoa *et al.*, 2007). The hydrocarbons are not sufficiently abundant for the sandstones to be considered a palaeo-reservoir, although they may have served as a migration conduit or carrier bed. Evidence of hydrocarbon migration has been found in syn-extensional limestones and shales in the DS1+2 and DS3 units in the central sector of the basin (Fig. 4n, o) (Omodeo-Salé and Suárez-Ruiz, 2017). Fractures in these units, now filled with calcite, are interpreed to have been formed as a consequence of the expulsion of hydrocarbons from competent layers originally rich in organic matter. The irregularity of the fractures results from variations in lithology (shaly organic-rich layers versus thin limestones and/or sandstones) (see Bordenave, 1993, Plates 1 and 2).

Petroleum system elements

Source rocks

Based on the data presented in Omodeo-Salé *et al.*, (2016), three units can be considered as source rocks for the Cameros Basin petroleum system (see Fig. 2a for locations):

- The Callovian Pozalmuro Formation (approximately 100 m thick), a sequence of alternating marly carbonates and black shales deposited in an outer platform setting under anoxic conditions (Mas *et al.*, 2002, 2003);
- The Berriasian Valdeprado Formation (~1000 m thick), composed of laminated marls and thick black shale intervals interpreted to have been deposited in shallow, perennial coastal lakes and surrounding mudflats with a restricted circulation. Black shales were deposited during a wet climate phase in anoxic conditions (Quijada *et al.*, 2013a, b; Quijada *et al*., 2016);
- The Enciso Group (~400 m thick, upper Barremian – lower Aptian), composed of dark fluvio-lacustrine mudstones deposited in coastal wetlands and lagoons with restricted circulation (Alonso-Azcárate, 1997; Alonso-Azcárate *et al.*, 1999; Mas *et al.*, 1993; Suárez-Gonzalez *et al.*, 2013).

These deposits are at present overmature and thus lean in organic carbon (Fig. 5; see Appendix 1, 2 and 3: page 169-171). However, the pyrobitumen particles dispersed in the matrix and the fine-grained residue (Fig. 4f-i) indicate that generation and/or migration of hydrocarbons has occurred in these units before their thermal over-maturation.

The immature deposits of the Abejar Formation (DS7),which crop out in the south of the basin, cannot be considered as a potential source rock despite their good hydrocarbon potential (Fig. 5a). This is because of the restricted thickness of the organic-rich intervals (cm to metre) and the resulting dilution of organic matter within the mostly siliciclastic succession.

Reservoirs

The continental-fluvial facies constituting the syn-extensional Cameros Basin includes potential sandstone reservoirs in a number of units (e.g. DS1+2 – Tera Group; DS3 – Huerteles Formation; DS7 – Urbión Group; and DS8 – Olivan Group). However, most of these deposits were affected by deep burial and/or intensive hydrothermal metamorphism, considerably reducing their porosity. In the Urbión Group sandstones, primary porosity may have been preserved due to the rigid grain framework (Arribas *et al.*, 2003; Arribas *et al.*, 2014; Ochoa *et al.*, 2007), making the sandstones a potential reservoir unit. Traces of hydrocarbons have been identified between quartz grains in these sandstones, which indicates the presence of oil in the pore spaces before quartz cementation occurred (Mantilla-Figueroa *et al.*, 1998; Ochoa *et al.*, 2007).

The shallower burial of the post-extensional deposits allowed higher porosities to be preserved than in the syn-extensional units. The lowermost sandstone unit, the Utrillas Formation, is at the present day impregnated with light to dark brown bitumen (Fig. 4c and d), and the unit can therefore be considered as a palaeo-reservoir. However, the areal extent of the bitumen impregnation in the subsurface is uncertain, and it is therefore not clear if the sandstones formed a reservoir unit or merely a carrier bed.

Seals and overburden rocks

The shales and limestones intercalated in the fluvial sandstone bodies of the Enciso Group could serve as a seal for the underlying Urbión Group reservoir, whereas the post-extensional Upper Cretaceous marl-limestone unit could be the seal for the Utrillas Formation reservoir (Mas *et al.*, 2003, 2011; Ochoa *et al.*, 2007). The entire syn-extensional stratigraphic record, together with the post-extensional deposits may act as overburden (Fig. 3).

MATERIALS AND METHODS

Conceptual geological model

In order to reconstruct the hydrocarbon generation and migration history in the Cameros Basin, available

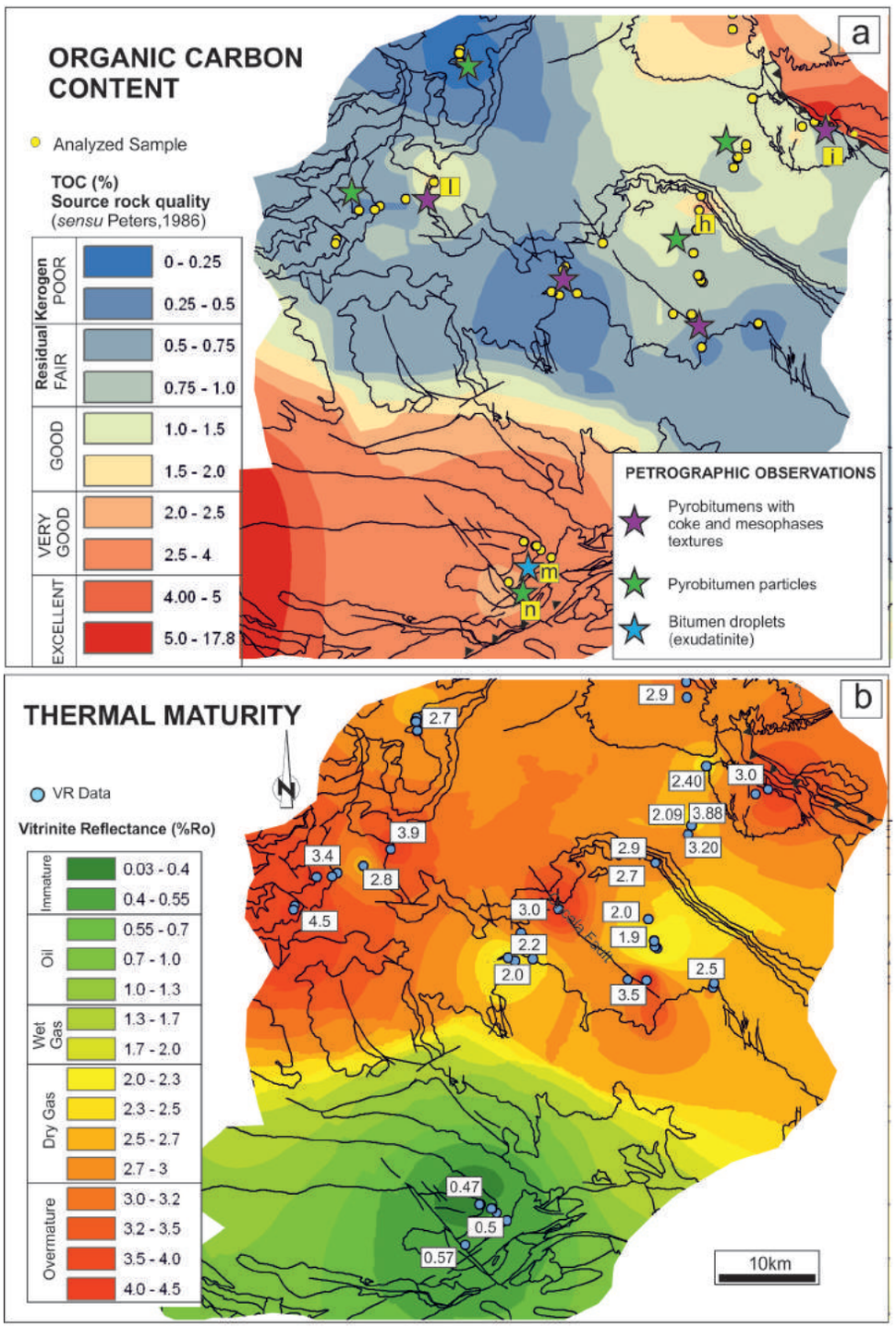

Fig. 5. (a) Map of the Cameros Basin showing the variation of the total organic carbon content (TOC, %) in the basin fill. TOC was measured in outcrop samples collected throughout the stratigraphic column (modified from Omodeo-Salé *et al.*, 2016). Letters indicate the location of the samples shown in Fig. 4. Limits of the geological units correspond to those shown in Fig. 2.
(b) Maturity map of the basin infill based on vitrinite reflectance measurements. Vitrinite reflectance was measured in outcrop samples collected throughout the stratigraphic column (modified from Omodeo-Salé *et al.*, 2016).

geological and geochemical data were integrated into a 2D thermal model built using PetroMod software (Version 2011, Schlumberger) including the TecLink 2D tool. In order to define the physical and temporal input necessary for modelling, a conceptual geological model of the basin was developed (c.f. Littke *et al.*, 2008; Tissot *et al.*, 1987; Welte and Yukler, 1981; Welte *et al.*, 1997). The geological model was based on a north-south balanced cross-section presented by Omodeo-Salé *et al.* (2014) (Fig. 2b), which was itself in general based on field observations and on available seismic and well data. To simplify the conceptual

Table 2. Depositional and erosional events defined in the conceptual model.

Age at the base (Ma)	Event no.	Event Type	Layer
0	24	Erosion	Paleo-Section 0Ma
17	23	Tectonic/Erosion	Paleo-Section 17Ma
22	22	Tectonic/Erosion	Paleo-Section 22Ma
29	21	Tectonic/Erosion	Paleo-Section 29Ma
36	20	Tectonic/Erosion	Paleo-Section 36Ma
43	19	Tectonic/Erosion	Paleo-Section 43Ma
50	18	Deposition	Cenozoic
50	17	Tectonic	Paleo-Section 50Ma
65.5	16	Hiatus	Hiatus 65.5_0
98	15	Deposition	Upp_Cretaceous
106.5	14	Deposition	Utrillas
108.7	13	Hiatus	Hiatus 108.7_106.5
121	12	Deposition	DS8
127	11	Deposition	DS7
129	10	Deposition	DS6
136.7	9	Deposition	DS5
142.3	8	Deposition	DS4
145.5	7	Deposition	DS3
150.8	6	Deposition	DS1+2
164.7	5	Deposition	Jurassic
205	4	Hiatus	Hiatus 205_164.7
245	3	Deposition	Triassic
380	2	Hiatus	Hiatus 380_245
500	1	Deposition	Basement

model, only the main thrust and back-thrust faults which limit the basin to north and south, respectively, were considered (Fig. 2b) whereas post-sedimentary vertical faults were omitted.

In order to model the evolution of the Cameros Basin in time, eight palaeo-sections were generated which represent a sequence of different geometries from the undeformed state at the end of the post-extensional stage to the present-day (Fig. 6). These sections were obtained by means of tectonic reconstructions and cross-section balancing using 2D-Move software (Version 2008, Midland Valley). The end-member section at 17 Ma corresponds to the balanced cross-section (Fig. 2b), and its restoration (65 Ma) takes into account northwards displacement along the main thrust of 30 km and southward displacement along the back-thrust of 3 km. The palaeo-sections were combined using the PetroMod TecLink 2D module. Each palaeo-section was split into individual fault blocks that retained their structural integrity during the model's tectonic evolution. The simulator first calculated the palaeo-sections, then integrated the results in an additional iteration step (IES, 2007).

To simulate the correct chronological basin history in the model, a consecutive sequence of depositional, non-depositional and/or erosional events were defined (Table 2). Depositional events were represented in the model by layers corresponding to pre-, syn- and post-extensional units (Figs. 2 and 3). The assigned lithologies were defined by sandstone, limestone and shale percentages (Table 3). The petrophysical properties of the mixed lithologies were proportionally calculated by the modelling package (Hantschel and Kauerauf, 2009).

Erosion

The most significant erosion event occurred during basin inversion (Eocene to Early Miocene), and little erosion took place during the preceding pre-, syn- and post-extensional stages. The thickness of the eroded section was estimated by stratigraphic and structural reconstructions (Mas *et al.*, 1993; Guimerà *et al.*, 1995; Muñoz-Jiménez and Casas-Sainz, 1997; Casas-Sainz and Gil-Imaz, 1998; Omodeo Salè *et al.*, 2014).

Table 3. Petrophysical properties assigned to the facies defined in the model.

Facies name	Lithology (%)			Initial Porosity (%)	Density (Kg m^{-3})	Permeability at porosity of (log mD)		Heat Capacity (Kcal kg^{-1} K^{-1})		Thermal Conductivity (W m^{-1} K^{-1})	
	Limestone	Sandstone	Shale			25%	45%	20ºC	100ºC	20ºC	100ºC
Cenozoic	0	95	5	42	2700	3	4.84	0.2	0.23	5.95	4.85
U. Cretac	60	20	20	51	2710	1	1.52	0.2	0.23	3	2.69
Utrillas Fm	0	80	20	40	2760	2	3.62	0.21	0.24	3.35	2.95
Oliván	5	70	25	49	2667	1.4	3.55	0.21	0.24	3.75	3.24
Enciso	45	20	35	51	2704	-0.36	1.10	0.21	0.24	2.13	2.05
Abejar	0	70	30	46	2700	1.7	4.37	0.2	0.23	4.21	3.58
Pantano	0	80	20	47	2684	1.8	3.88	0.21	0.24	3.74	3.23
Golmayo	40	40	20	51	2700	0.89	2.09	0.2	0.24	2.54	2.35
Urbión	0	60	40	53	2664	0.6	2.93	0.21	0.24	3.73	3.22
Valdeprado	60	4	36	55	2670	-0.81	0.28	0.21	0.24	2.01	1.96
Huerteles	15	35	50	50	2714	1.2	2.97	0.2	0.24	3.03	2.71
Tera	5	60	35	51	2673	0.76	3.48	0.21	0.24	3.37	2.96
Jurassic	100	0	0	51	2680	0.73	1.00	0.2	0.23	2	1.96
Triassic	Evaporite			10	2540	-	-	0.19	0.21	4.69	3.91
Basement	Mafic/Granitic Rock			5	2750	-	-	0.19	0.22	2.72	2.35

A maximum eroded thickness of 5500 m has been determined in the central part of the basin, gradually decreasing toward the south (Fig. 2b).

The simulation of erosion in the petroleum system model required the sequential removal of layers in reverse order of deposition (Poelchau *et al.*, 1997). In general, this is an acceptable simplification in weakly deformed and regionally uplifted sedimentary basins, but it is not acceptable in overthrust systems such as the Cameros Basin where units of different ages were eroded simultaneously. To overcome this problem, partially eroded retro-deformed balanced cross-sections were used to construct the model (Fig. 6). Progressive erosion of the uplifted units was considered.

Boundary conditions and thermal calibration data

The most important boundary condition defined in the model is the variation through time of the heat flow at the base of the model (11 to 13 km deep). Because of the continental nature of most of the deposits, sea-level fluctuations and resulting palaeo water depth corrections were not considered. The sediment-water interface temperature (SWIT) was calculated by the software specific routine, which defines the evolution temperature at sea level considering variations of global mean surface temperature and latitudinal variation of the study area through time (Wygrala, 1989)

The heat flow maximum in the Cameros Basin was estimated considering the magnitudes of the initial and thermal subsidence recorded by applying the approach of Royden (1986). The maximum heat flow in an extensional basin occurs at the end of mechanical lithosphere stretching (initial subsidence) and before thermal relaxation (thermal subsidence), at the time when the asthenosphere is at its shallowest (McKenzie, 1978; Royden and Keen, 1980; Royden, 1986; Allen and Allen, 2017). Initial and thermal subsidence data values were measured along the basin and plotted on the graphs proposed by Royden (1986), which related the subsidence to crustal and lithosphere stretching factors. By this method a maximum heat flow value of 65 mW/m² at the end of the extensional stage was calculated (Omodeo-Salé *et al.*, 2017).

For the model, a heat flow trend was proposed which had a maximum value of 65 mW/m² at the end of the syn-rift stage subsequently decreasing to 60 mW/m² in the post-rift stage (Fig. 7a). The latter heat flow was maintained until 0 Ma and corresponds to the present-day heat flow of 60 mW/m^2 measured in wells in the area (Fernández *et al.*, 1998). The model was thermally calibrated against measured vitrinite reflectance derived from previous studies (Omodeo-Salé *et al.*, 2016; 2017), using the Sweeney and Burnham (1997) kinetic model. Vitrinite reflectance (Ro%) was measured in 72 organic-matter rich outcrop samples, representative of the entire stratigraphic record of the basin (Fig. 5b, and Appendix 1 and 3).

Source rock properties

The three source rock intervals considered are at present overmature (Fig. 5b). Thus, the original type of organic matter present was inferred on the basis of the interpreted depositional environments (see above): Type II kerogen was assigned to the Pozalmuro Formation marine black shales; Type I kerogen to the Valdeprado Formation black shales; and Type III kerogen to the Enciso Group wetland deposits (Table 4).

Table 4. Geochemical and kinetic parameters assigned to the source rocks defined in the model. PSR = Pozalmuro source rock; VSR = Valdeprado source rock; ESR = Enciso source rock.

Source Rock	TOC [%]	HI [mg HC/g TOC]	Kerogen Type	Compositional Kinetic	Capillary pressure Petroleum-Water [MPa]		
					70% porosity (PSR) 53% porosity (VSR, ESR)	25% porosity	5% porosity
PSR	8	730	Type II	Ungerer TII (NS)	0	0.24	1.6
VSR	17	710	Type I	Pepper and Corvi TI	0	0.1	0.5
ESR	2.8	170	Type III	Pepper and Corvi TIII	0	0.1	0.4

The geochemical parameters (initial TOC content, HI index, and kinetics) of immature high-TOC intervals within the siliciclastic succession outcropping in the south of the basin (DS7 unit, Abejar Formation) were used to define the original properties of the source rocks, which are at present overmature. The marine Pozalmuro Formation lacks an immature analogue in the basin; therefore, the geochemical parameters of Lower Jurassic source rocks in the Ayoluengo oilfield (located near Burgos in northern Spain, about 200 km from the central part of the Cameros Basin) were used because they were deposited in a similar marine setting (Sanz, 1967; Abeger *et al.*, 2003; Permanyer *et al.*, 2013).

In order to simulate the thermal transformation of kerogen over time, the kinetics proposed by Ungerer (1990) and Pepper and Corvi (1995) were assigned. Kinetics were chosen considering the type of original kerogen present (Table 4).

Hydrocarbon migration in the source rock was calculated using a multi-phase Darcy flow. The capillary pressures for the petroleum–water system were calculated for the defined lithologies at different porosities using a bilinear interpolation scheme (Table 4) (Hantschel and Kauerauf, 2009). In basin modelling, no distinction is made between primary migration in source rocks and secondary migration in reservoir and carrier rocks because hydrocarbon migration is considered as a flow of hydrocarbons through the free pore space (Hantschel and Kauerauf, 2009).

RESULTS AND DISCUSSION

Thermal history

The proposed heat flow (Fig. 7a, blue curve) is validated only in the southern sector of the basin, where vitrinite reflectance data fit the calculated curve (calibration well 1) (Fig. 7b). However, in the central and northern sectors (calibration wells 2, 3 and 4), vitrinite reflectance measurements indicate that higher heat flow values were recorded than those calculated in the initial scenario (blue curve in Fig. 7b). Furthermore, the highest values were measured in shallower stratigraphic intervals, inverting the typical maturity-depth trend, which should increase with progressive burial. This anomaly has been interpreted to be caused by the circulation of hydrothermal fluids (Omodeo-Salé *et al.*, 2017, 2016), rising from deep crustal detachment faults with temperatures of more than 300 °C (Casquet *et al.*, 1992; González-Acebrón *et al.*, 2011).

To reproduce the effects of hydrothermal circulation in the current thermal model is not straightforward. Petroleum system modelling software can only simulate conductive heat transport from the bottom to the top of a basin fill (Büker *et al.*, 1995; Poelchau *et al.*, 1997; Yalçin *et al.*, 1997) and the effects of advective heat transport due to the circulation of high-temperature fluids can only be approximated. To simulate thermal events occurring over a relative short time span (e.g. due to dike intrusion or the circulation of hydrothermal fluids), one solution is to add heat-flow peaks in the basal heat-flow history (Taylor *et al.*, 1998). In order to simulate the two hydrothermal events recognized in the Cameros Basin, two heat-flow peaks of short duration (1 Ma) at 85 Ma and 45 Ma were added to the basal heat-flow history curve in the central and northern sectors (Fig. 7a, red curve). The addition to the two heat-flow peaks improved the model calibration, as the calculated curves fit much better the highest measured $\%R_o$ values (red curves in Fig. 7b). However, the high $\%R_o$ values measured in the shallow stratigraphic intervals ($\%R_o \sim 3$) and the anomalously decreasing $\%R_o$-depth trend of the measured data in the central-northern sector of the basin cannot be reproduced. But taking into account the software-related limitations on conductive heat transport, the fact that basal heat flow peaks affect the entire model by definition and that calibration data are only from outcrop samples, the calibration proposed can be considered as the best approximation.

Hydrocarbon generation, migration and accumulation processes

The model determined the timing of source rock maturation, the kerogen transformation ratios and the timing of hydrocarbon expulsion (Figs 8 and 9). Migration pathways were in general reconstructed

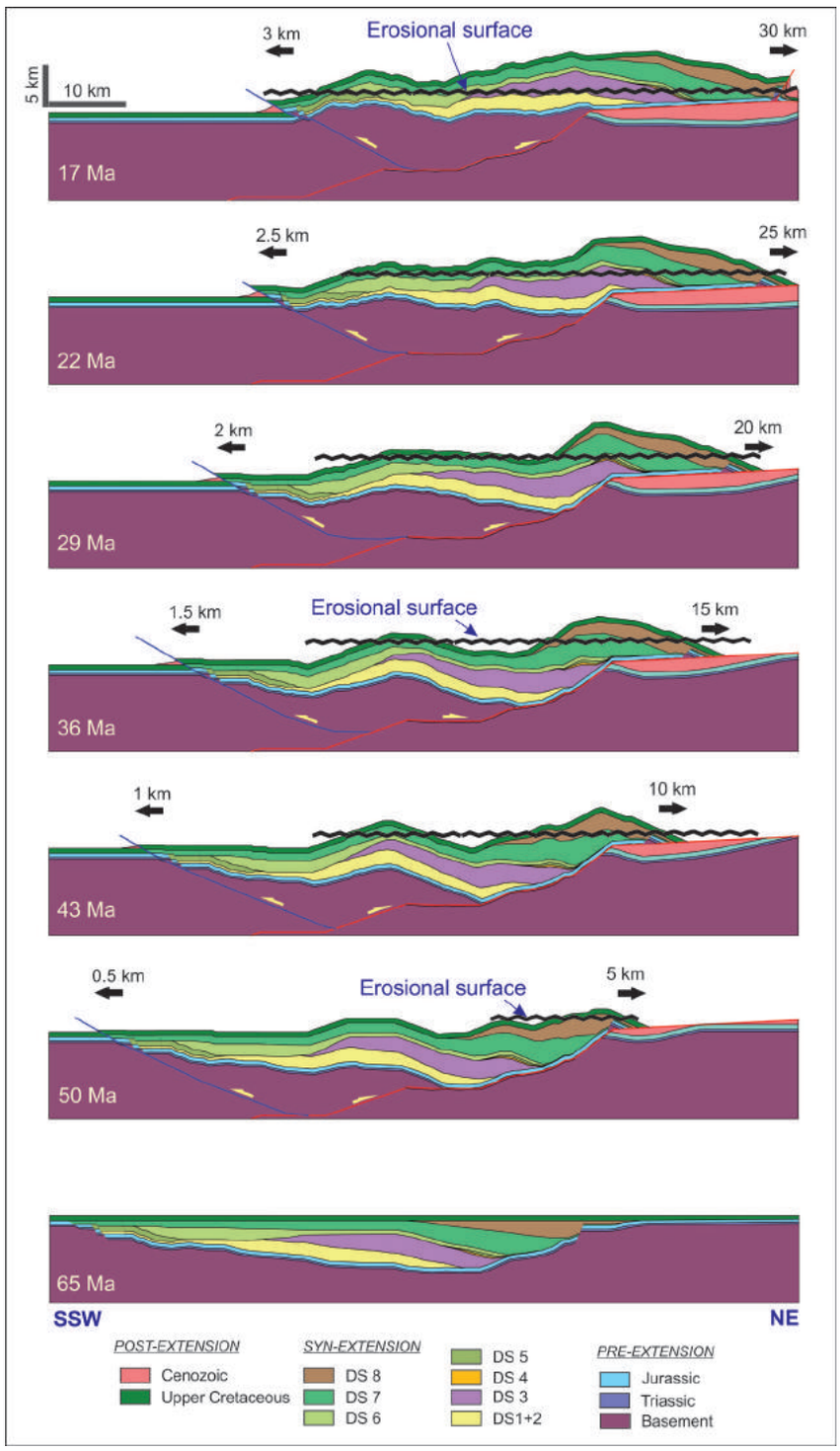

Fig. 6. Modelled cross-sections of the Cameros Basin showing the basin evolution over time from the undeformed state (65 Ma) to the end of the inversion phase (17 Ma). End-member sections from Omodeo-Salé *et al.* (2014). The erosional surface during inversion was estimated in order to generate the model input sections. (Modified from Omodeo-Salé, 2014).

taking into account the permeability of the stratigraphic units together with their geometric variation through time (Fig. 10).

In the early part of the extensional phase (142.3 – 136.7 Ma), the Pozalmuro source rock and the most deeply buried parts of the Valdeprado source rock are modelled to have entered the oil window, as a consequence of the deposition of the overburden units DS1+2 – DS4, and initial hydrocarbon expulsion occurred. The generated hydrocarbons migrated vertically, toward the topographic surface.

During the intermediate part of the extensional stage (136.7 – 121 Ma), the entire Valdeprado source rock reached the oil window as a consequence of the deposition of the very thick DS7 unit (Fig. 8). The Pozalmuro source rock began to enter the wet-gas

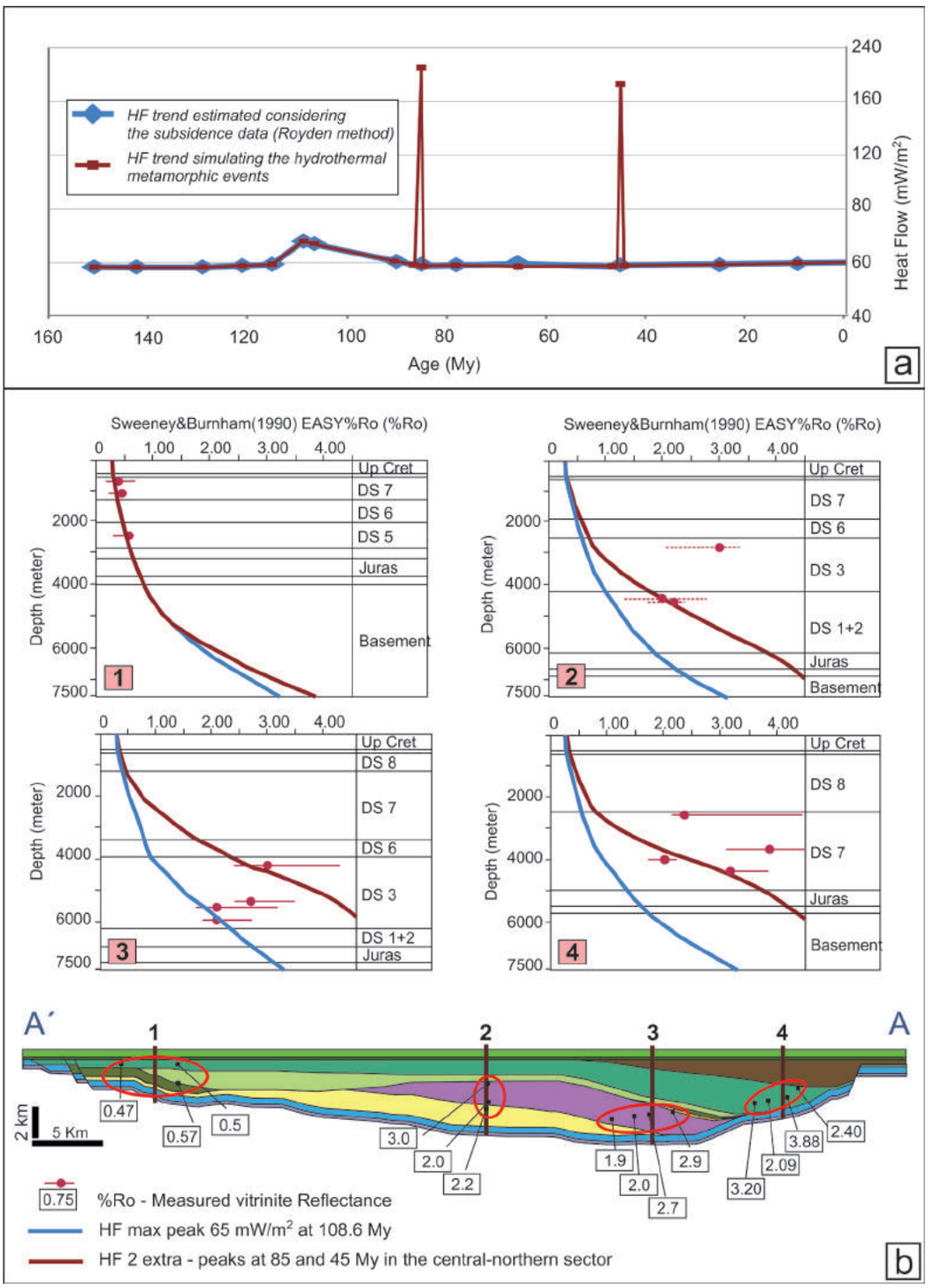

Fig. 7. (a) Basal heat flow history (mW/m²) used in the model. The first scenario (blue curve) is characterized by a single maximum heat flow peak of 65 mW/m² at the end of the extensional phase consistent with the subsidence history of the basin. In the second scenario (red curve), two additional short-time peaks at 85 and 45 Ma were added to reproduce the effects of heating due to hydrothermal fluid circulation.
(b) Calibration of the 2D thermal model using the two proposed heat-flow scenarios with measured vitrinite reflectance data (modified from Omodeo-Salé *et al.*, 2017). The cross-section at the bottom shows the location of extracted pseudo-wells used to calibrate the model and illustrated above (1, 2, 3 and 4), and the projection of measured data into the section.

window in the central part of the modelled section, and was in the oil window towards the margins of the profile (Fig. 8). According to the model, migration from the Pozalmuro and Valdeprado source rocks occurred upwards towards the surface throughout the overlying carrier rocks and laterally to the south (Fig. 10). A significant hydrocarbon flow path developed through the sandstones of the Urbión Group (DS4, DS5, DS6, and DS7 units) in the central-northern sector of the basin and remnants of bitumen have been found in

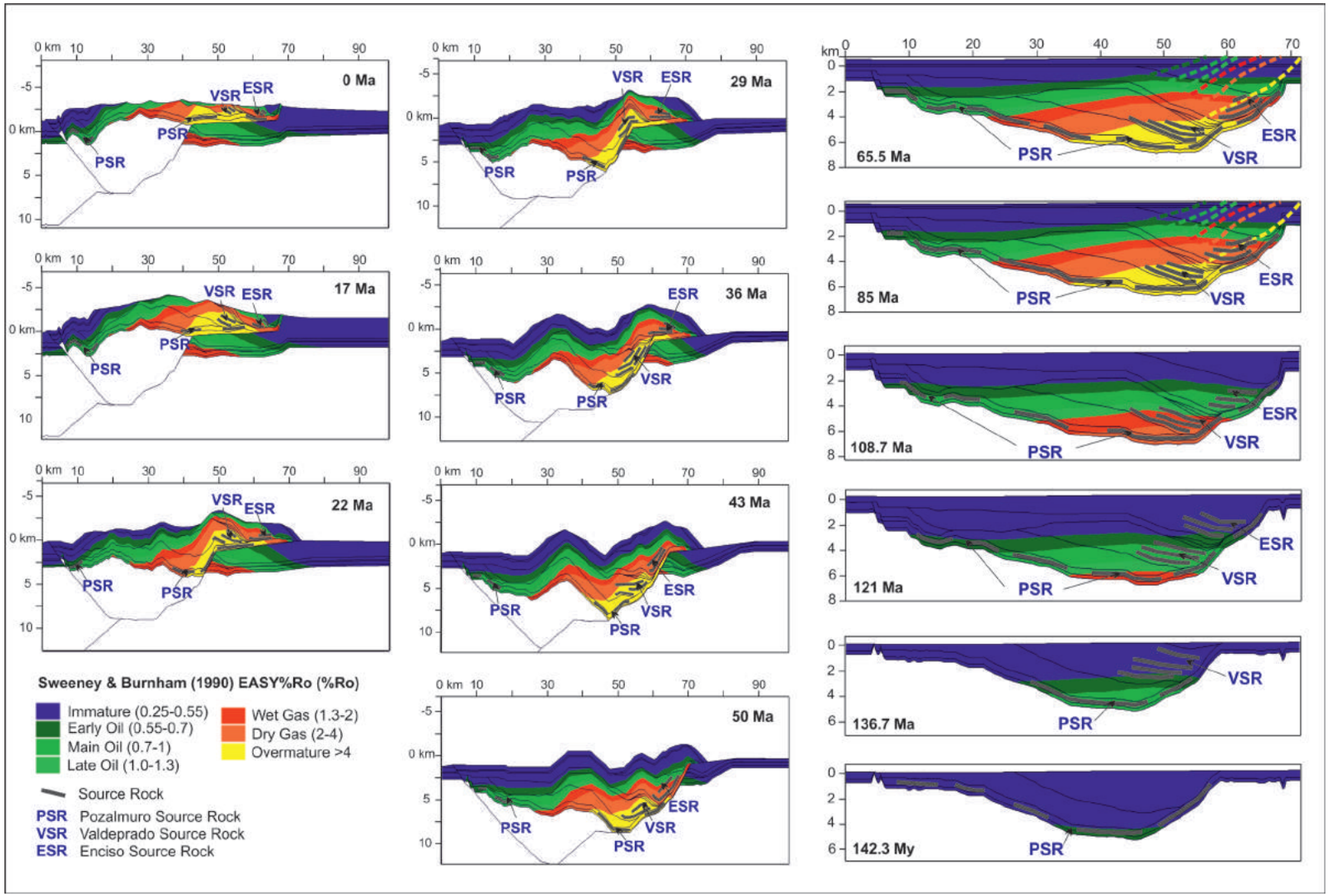

Fig. 8. Reconstruction of the thermal maturity of the basin infill through time. The colour scheme shows the maturity evolution along the profile. To reproduce the effects of the circulation of hydrothermal fluids in the northern part of the basin, higher thermal conditions needed to be considered in the uppermost stratigraphic layers in that area at the end of the post-extensional stage (85 and 65.5 Ma) which are indicated by the dashed lines. In the inverted sections, vertical exaggeration with respect to the original sections in Fig. 6 is 1:2. Source rocks are indicated in each section: PSR, Pozalmuro source rock; VSR, Valdeprado source rock; ESR, Enciso source rock.

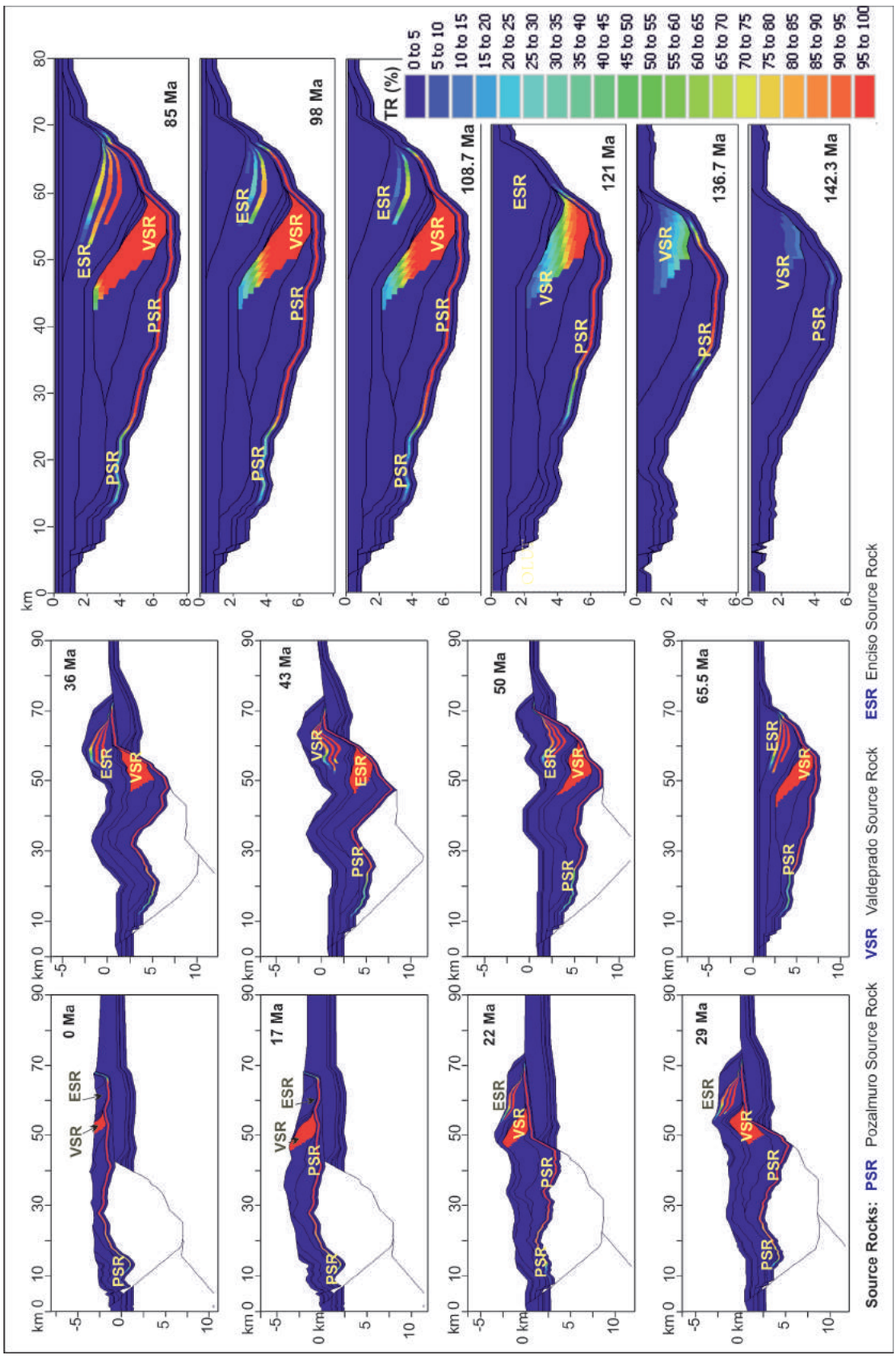

Fig. 9. Plots showing the modelled evolution of the transformation ratio (TR %) of kerogen initially present in the potential source rocks of the Cameros Basin through time. In the inverted sections, vertical exaggeration with respect to the original sections in Fig. 6 is 1:2. Source rocks are indicated in each section: PSR, Pozalmuro source rock; VSR, Valdeprado source rock; ESR, Enciso source rock.

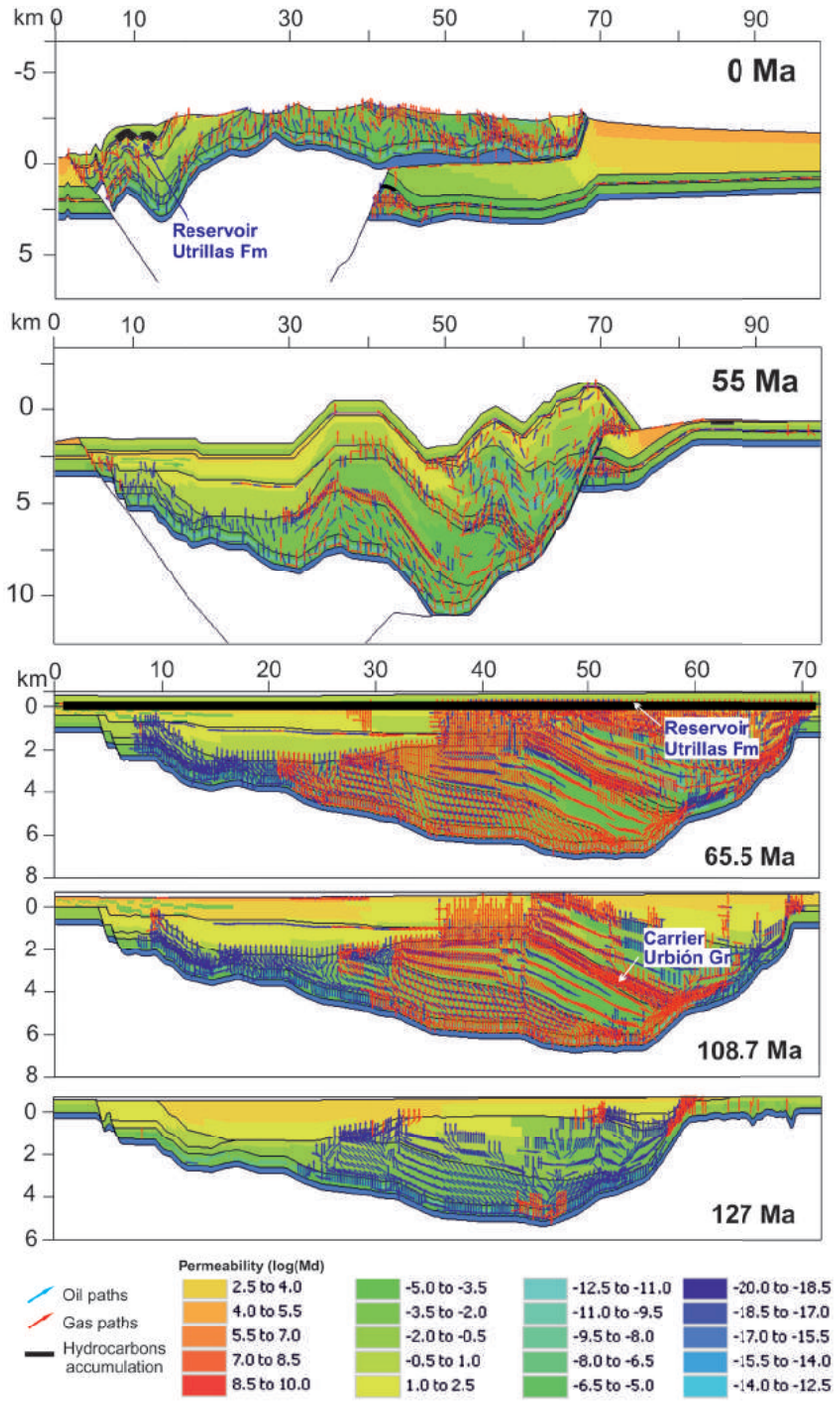

Fig. 10. Reconstruction of hydrocarbon migration pathways and oil/gas accumulations through time. In the inverted sections, the vertical exaggeration with respect to the original sections in Fig. 6 is 1:2.

these units (Mantilla-Figueroa *et al.*, 1998; Ochoa *et al.*, 2007). However, hydrocarbons did not accumulate in significant volumes because of the absence of a seal and/or traps (Fig. 10). Thus, no hydrocarbon accumulations formed in the Urbión Group.

In the latest part of the extensional stage (121–108.7 Ma), the Pozalmuro source rock entered the gas window in the central-northern part of the modelled section as a consequence of the deposition of the DS8 overburden unit, whereas it remained in the oil window in the south of the basin (Fig. 8). In this phase, most of the Valdeprado source rock was in the gas window with an almost complete transformation of kerogen into hydrocarbons (Figs 8 and 9). In this phase, the peak generation of hydrocarbons occurred (127–108.7 Ma) (Fig. 11), with a transformation ratio up to 50-90% (Fig. 9). The Enciso source rock entered the oil window at 108.7 Ma with the partial transformation of kerogen (Fig. 9). Hydrocarbon generation then declined after 108.7 Ma (Fig. 11) because most of the kerogen had

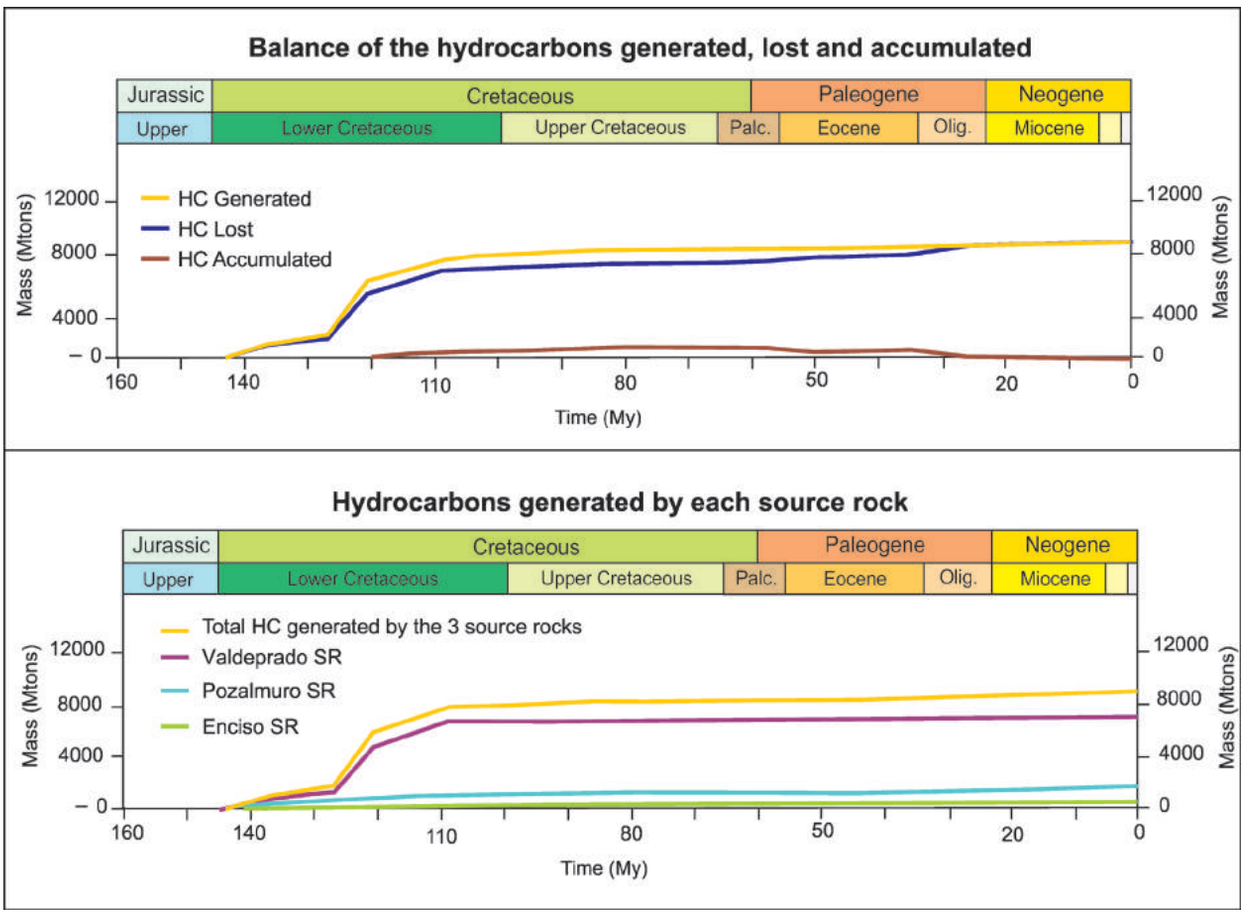

Fig. 11. Chart showing hydrocarbon generation, accumulation and loss through time in the Cameros Basin.

already been transformed into oil and gas (Fig. 9). In the central-northern sector, gas migrated through the Urbión Group and along syn-sedimentary faults. In the south of the basin, the hydrocarbons expelled from the Pozalmuro source rock migrated upwards through the DS1+2, DS5, DS6 and DS7 units (Fig. 10). The overmature hydrocarbons found in the more immature shallower deposits (DS7 unit, Abejar Formation) support this migration event as reconstructed by the model. Most of the hydrocarbons generated at this stage were lost to the surface due to the absence of a seal (Fig. 10).

In the post-extensional stage (108.7 – 65.5 Ma), the regional thermal event (≈ 85 Ma) caused the complete thermal transformation and alteration of organic matter – including both kerogen in the Pozalmuro, Valdeprado, and Enciso source rocks (Fig. 8 and Fig. 9), and hydrocarbons accumulated in reservoirs. Because of the difficulty in correctly reproducing the effects of the circulation of hot hydrothermal fluids in the model, overmature thermal conditions were not correctly calculated. However, they were assumed to occur in the shallowmost stratigraphic intervals relative to those calculated by the model (Fig. 8, see the lines drawn in the 85 and 65.5 Ma sections). The alteration textures in pyrobitumen particles observed in units outcropping at the northern basin margin (Fig. 4g and h) are interpreted to result from this abrupt thermal event.

Oil and gas generated in the post-extensional phase accumulated in the sandstones of the Utrillas Formation (Fig. 10). These accumulations probably consisted mainly of gas because the Pozalmuro, Valdeprado and Enciso source rocks were in general in the gas window at that time (Fig. 8). In the central-northern sector of the basin, the Valdeprado source rock is the most important source rock unit by volume of petroleum generated (Fig. 11), due to its high productivity and thickness (Table 4 and Fig. 2b). The lesser thicknesses of the Pozalmuro and Enciso source rocks together with their relatively lower hydrocarbon potential (Table 4) resulted in the generation of smaller volumes of hydrocarbons (Fig. 11). The inversion of the basin (50-17 Ma) caused the gradual erosion and destruction of the reservoirs formed in the northern sector of the basin.

The southern sector of the basin underwent a different tectonic evolution which resulted in different source rock maturation and hydrocarbon generation histories. The low subsidence rates recorded in this part of the basin resulted in a later onset of hydrocarbon generation and expulsion at the end of the syn-

Table 5. Elements of the petroleum systems (PS) identified.

Elements and Processes	PS1	PS2	PS3	PS4
Source Rock	Pozalmuro Fm (central-northern sectors)	Valdeprado Fm	Enciso Gr	Pozalmuro Fm (southern sector)
Reservoir	Utrillas Fm	Utrillas Fm	Utrillas Fm	Utrillas Fm
Seal	Upper Cretaceous	Upper Cretaceous	Upper Cretaceous	Upper Cretaceous
Migration-Generation-Accumulation timing	Syn-extensional phase	Middle-late syn-extensional phase	Late syn-extensional and post-extensional phases	Post-extensional and inversion phases
Trap	Stratigraphic	Stratigraphic	Stratigraphic	Structural
Overburden units	DS1+2-DS8; UpperCretaceous	DS4-8; UpperCretaceous	DS8; UpperCretaceous	DS1+2, DS5-DS7; Upper Cretaceous

extensional stage (121 Ma), when the Pozalmuro source rock entered the oil window as a consequence of the deposition of the DS7 and Upper Cretaceous units (Fig. 8). Unlike the rest of the basin, hydrocarbon generation and accumulation continued in the southern sector until the last part of the inversion phase (late Oligocene, 30-23 Ma) because the source rock in this area was still in the oil generation window. In addition, the basin was not completely uplifted and eroded (Figs 8 and 9) preserving some remaining potential in the Pozalmuro source rock (Fig. 11).

Formation of traps

During the entire syn-extensional phase, due to the absence of regionally extensive impermeable units (seals) and because of compressive tectonic activity, no relevant stratigraphic and structural traps formed. Thus, most of the hydrocarbons generated in this phase were lost (Fig. 11). In the post-extensional phase, the deposition of the impermeable Upper Cretaceous marlstones provided an effective seal and resulted in the accumulation of hydrocarbons in the underlying sandstone of the Utrillas Formation (Fig. 10).

During the inversion phase (50–17 Ma), small volumes of hydrocarbons probably accumulated in structural traps formed at that time. However, the continuous uplift of the basin prevented the preservation of these palaeo accumulations, exposing and eroding them quickly at the surface (Fig. 10). In contrast, in the southern sector of the basin, small-scale fold-related traps may have been preserved as a consequence of the reduced uplift rate. Thus, hydrocarbons were trapped in the gentle anticlines formed in this area (Fig. 10). Modelling results indicate that the principal reservoir formed in the sandstones of the uppermost Utrillas Formation (Fig. 10) which is in agreement with the observation of bituminous sandstones in the Utrillas Formation in an outcrop location near the village of Fuentetoba (Figs 4a-e).

The results presented here indicate that the main cause of the scarcity of hydrocarbons accumulations in the Cameros Basin is the lack of synchroneity between fluid expulsion and traps formation. Uplift, erosion and subaerial exposure of the few accumulations which were formed was a secondary cause.

Petroleum systems evolution

In the Cameros Basin, four different petroleum systems can be considered, each including an active source rock (Fig. 12 and Table 5) (*sensu* Magoon and Dow, 1994). In the case of the Pozalmuro source rock, two different petroleum systems were developed as this source rock became mature at different times and in different sectors of the basin. For each petroleum system, the critical moment was defined as the time of peak kerogen transformation into hydrocarbons. The interval of time when hydrocarbons could be preserved in the reservoir if traps were present was defined as the preservation time. The preservation of a petroleum system can be terminated by uplift, faulting, erosion and/or the occurrence of significant thermal events.

The first two petroleum systems activated in the basin are related to the Pozalmuro and Valdeprado source rocks (Fig. 12). In both cases, the critical moment was at 108.7 Ma when peak kerogen transformation to hydrocarbons occurred. The critical moment does not overlap with the time of preservation and most of the hydrocarbons generated were therefore lost because of the absence of a seal and/or trap during the time of maximum generation and migration.

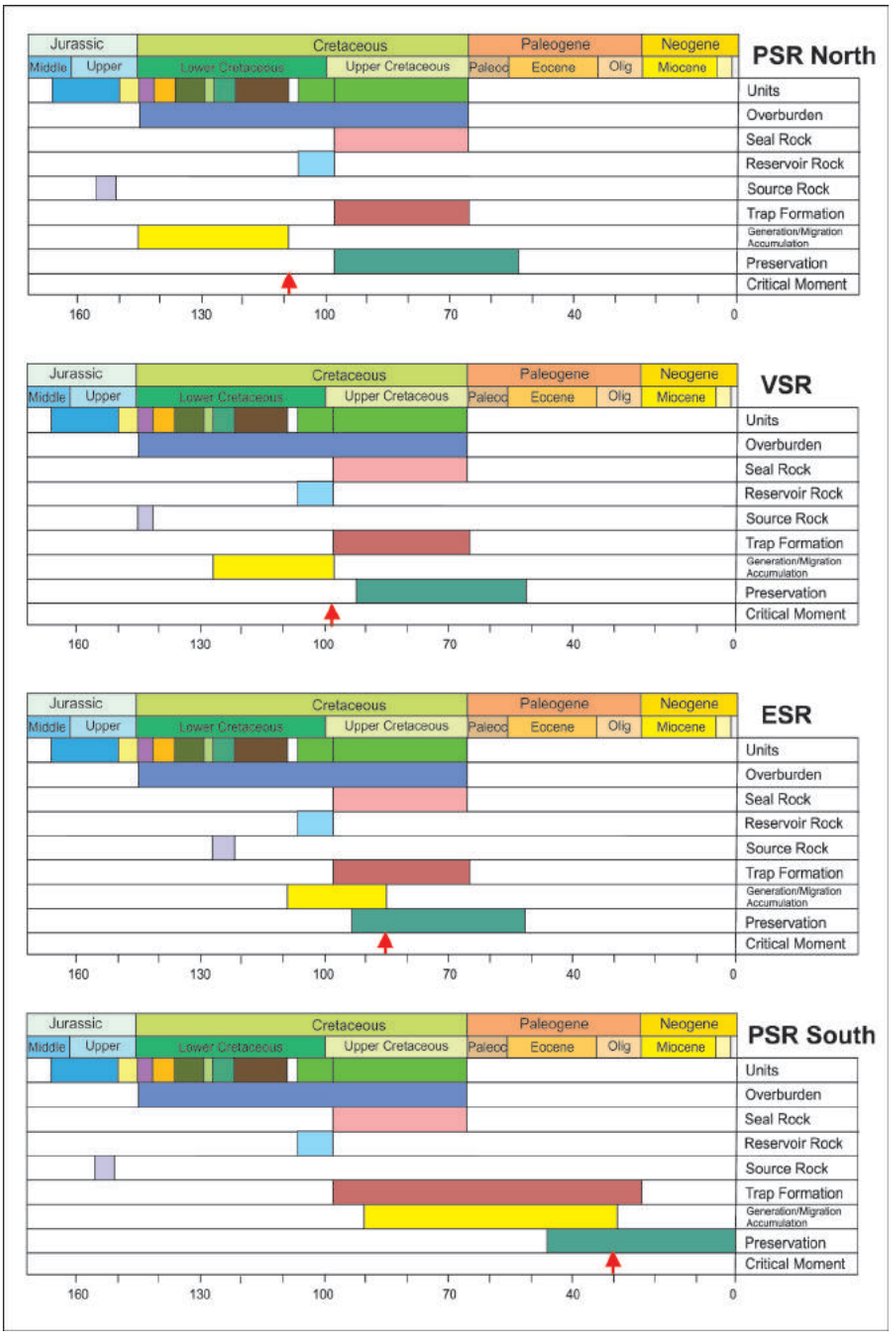

Fig. 12. Petroleum systems chart of the Cameros Basin (*sensu* Magoon and Dow, 1994) indicating the petroleum system elements (source rock, reservoir, seal), the timing of hydrocarbon generation, migration and accumulation, and the critical moment. PSR = Pozalmuro source rock; VSR = Valdeprado source rock; ESR = Enciso source rock

In the petroleum system corresponding to the Enciso source rock, hydrocarbon generation reached a peak at 85 Ma (Fig. 12). The critical moment coincides with the preservation time, and hydrocarbons generated therefore accumulated in reservoirs. However, the system was only preserved until the Eocene when the basin was uplifted and the traps were eroded.

The petroleum system corresponding to the Pozalmuro source rock located in the southern sector of the basin was active in the post-extensional and inversion stages when structural traps had already been created (Fig. 12). The critical moment occurred at around 30 Ma when the transformation ratio reached a maximum. Hydrocarbons accumulations were preserved until uplift of the basin at 17 Ma (Fig. 6).

Model assumption and result uncertainties

Reconstructing the hydrocarbon generation and accumulation history of an inverted and overthrused basin is a complex and somewhat uncertain undertaking due to problems of missing basin infill and subaerial exposure due to the tectonic uplift and erosion. The overmature thermal state of the original source rocks adds further difficulties for reconstructing the original

hydrocarbon potential in the area. Therefore, several assumptions had to be made, resulting in uncertainties of the model results.

Migration and accumulation processes: The use of a 2D section, instead of a 3D model, strongly limits the accurate evaluation of the hydrocarbon migration paths and accumulations. Furthermore, the section used herein represents only the central-eastern part of the basin and the western sector was not considered. Thus in order to properly evaluate the evolution of the entire petroleum system of the basin, further structural and geochemical data should be collected and integrated into a 3D petroleum system model.

Source rock maturation: Uncertainties in the erosion estimates can provide errors in the evaluation of the source rock maturation state and timing. The sedimentary thickness eroded during the inversion of the basin has been estimated by geometrical and structural reconstructions, which can result in under/over-estimation. The uncertainty connected to the reconstruction of deformation and erosion is of little relevance for modelling source rock maturity and hydrocarbon generation because maximum burial and additional heat input by hydrothermal events occurred before the inversion phase of the basin.

Thermal model calibration: outcrop samples were used to obtain temperature calibration parameters ($\%R_o$), necessary to validate thermal modelling, as subsurface well data were not available. Although altered and oxidized samples were carefully avoided for vitrinite reflectance measurements, possible errors due to weathering and/or contamination of the samples need to be taken into account. However, the vitrinite reflectance data are supported by other thermal indicators (fluid inclusion, mineral paragenesis, low thermochronology etc.; see references cited above), which also indicate high anomalous thermal conditions in the northern sector of the basin.

Hydrocarbon volume estimation: Due to the present-day overmature state of the source rocks, their original amount and type of organic matter can only be estimated by considering the properties of the few analogous immature deposits outcropping in the southern sector of the basin. Quantitative estimation of the hydrocarbons generated and accumulated in the basin was not therefore part of the project, whereas qualitative and relative estimates can be considered more reliable (Fig. 11).

Considering the assumptions necessary to synthesize the model input data for an inverted, eroded and partially overmature basin, uncertainties in the model results are inevitable. However, the results obtained in this work provide a sound reconstruction of the evolution of the petroleum system of the Cameros Basin and are consistent with the available geological data.

CONCLUSIONS

This study reconstructed the hydrocarbon generation, migration and accumulation history in the Cameros Basin, north-central Spain, by integrating available geological, structural, thermal, petrographic and geochemical data. Factors that have prevented the accumulation and preservation of commercial volumes of hydrocarbons were investigated.

The source rocks identified in the basin are at present overmature, but observations suggest that they have generated and expelled hydrocarbons in the past. In the northern sector of the basin, the Pozalmuro source rock (Callovian) entered in the oil window in the Early Berriasian and the Valdeprado source rock (Early Berriasian) in the Early Barremian, marking the onset of hydrocarbon generation which reached a peak in the Late Barremian – Early Albian (127–108.7 Ma). At this time, the Valdeprado source rock was the most important source rock by volume of petroleum generated. However, due to the absence of seals and/or traps, most of the hydrocarbons generated were not preserved. Potential traps formed only in the post-extensional stage when the deposition of carbonates and shales throughout the basin sealed the system. However, uplift and erosion of the basin during the inversion stage prevented the preservation of reservoir units. Hydrothermal activity in the northern sector of the basin may also have contributed to the failure of the Cameros Basin petroleum system to preserve accumulations by over heating and thereby thermally degrading the trapped petroleum.

In the southern sector of the basin, the generation of hydrocarbons began at the end of the syn-extensional stage (121 Ma) by the Pozalmuro source rock (Callovian in age and constituting part of the basin substratum). Unlike the rest of the basin, hydrocarbon generation and accumulation continued until the very early phase of inversion, because in this area the source rock was still in the generation window and the basin was not completely uplifted and eroded. The expelled hydrocarbons accumulated in the post-extensional Utrillas Formation sandstones and are at present still preserved in outcrops in the form of biodegraded bitumen.

ACKNOWLEDGEMENTS

Funding for this research was provided by the Spanish project grants CGL2008- 01648/BTE, CGL2008-04916/BTE, CGL2011-22709 and CGL2014-52670-P of the UCM-CM (Universidad Complutense Madrid Community). The petrographic and geochemical analyses were performed at the INCAR-CSIC laboratory (Oviedo, Spain), thanks to Isabel Suárez-Ruiz. Schlumberger is thanked for providing an

academic license for the PetroMod software.JPG editorial staff assisted with the English language presentation We thank L. B. Magoon for an initial constructive review of the paper. We would like to express our gratitude to Roger Baudino and an anonymous referee for their reviews of an earlier version of the manuscript.

REFERENCES

ABEGER, G., FERNANDEZ, A.J., SERRANO, A., QUESADA, S., VALLAURE, T., VARELA, J. and DEL OLMO, W. M., 2003. Petroleum Geology of the Oil and Gas Commercial Discoveries in Spanish Basins: Onshore Cantabrian basin. *2003 AAPG International Conference & Exhibition Technical Program*.

ALLEN, P. A. and ALLEN, J. R., 2017. Basin analysis: principles and applications. Blackwell, Oxford, 549 pp.

ALONSO, A. and MAS, J. R., 1993. Control tectónico e influencia del eustatismo en la sedimentación del Cretácico inferior de la Cuenca de Los Cameros. *Cuadernos de Geología Ibérica*, **17**, 285-310.

ALONSO-AZCÁRATE, J., 1997. Evolución de los filosilicatos y génesis de los yacimientos de pirita: su relación con las facies sedimentarias y el metamorfismo en la Cuenca de Cameros. Cretácico inferior. La Rioja-Soria. Doctoral Thesis, Universidad Complutense de Madrid, 544 pp.

ALONSO-AZCÁRATE, J., RODAS, M., BOTTRELL, S.H., RAISWELL, R., VELASCO, F. and MAS, J.R., 1999. Pathways and distances of fluid flow during low-grade metamorphism: evidence from pyrite deposits of the Cameros Basin, Spain. *Journal of Metamorphic Geology*, **17**, 339-348.

ALONSO-AZCÁRATE, J., RODAS, M., MAS, R. and VELASCO, F., 1995. Origen de las piritas de la cuenca de Cameros, (La Rioja). *Geogaceta*, **18**, 180-183.

ARCHE, A. and LÓPEZ-GÓMEZ, J., 1996. Origin of the Permian-Triassic Iberian Basin, central-eastern Spain. *Tectonophysics*, **266**, 443-464.

ARRIBAS, J., ALONSO, Á., MAS, R., TORTOSA, A., RODAS, M., BARRENECHEA, J.F., ALONSO-AZCÁRATE, J. and ARTIGAS, R., 2003. Sandstone Petrography of Continental Depositional Sequences of an Intraplate Rift Basin: Western Cameros Basin (North Spain). *Journal of Sedimentary Research*, **73**, 309-327.

ARRIBAS, J., GONZÁLEZ-ACEBRÓN, L., OMODEO-SALÈ, S., MAS, R., 2014. The influence of the provenance of arenite on its diagenesis in the Cameros Rift Basin (Spain). *In*: Sediment provenance studies in hydrocarbon exploration and production. Scott, R.A. *et al.* (Eds). *Geol. Soc. Lond., Spec. Publ.*, **386**, 63-73.

AURELL, M. and MELENDEZ, A., 1993. Sedimentary evolution and sequence stratigraphy of the Upper Jurassic in central Iberian Chain, northeast Spain,. In: POSAMENTIER, H. W., SUMMERHAYES, C. P., HAQ, B. U. and ALLEN, G. P. (Eds), Sequence stratigraphy and Facies Associations. *International Association of Sedimentologists, Special Publication*, **18**, 343-368.

BÁDENAS, B. and AURELL, M., 2001. Kimmeridgian palaeogeography and basin evolution of northeastern Iberia. *Palaeogeography, Palaeoclimatology, Palaeoecology*, **168**, 291-310.

BARRENECHEA, J.F., RODAS, M., FREY, M., ALONSO-AZCÁRATE, J. and MAS, J.R., 2001. Clay diagenesis and low-grade metamorphism of Tithonian and Berriasian sediments in the Cameros Basin (Spain). *Clay Minerals*, **36**, 325-333.

BARRENECHEA, J.F., RODAS, M. and MAS, J.R., 1995. Clay mineral variations associated with diagenesis and low-grade metamorphism of Early Cretaceous sediments in the Cameros Basin, Spain. *Clay Minerals*, **30**, 119-133.

BENITO, M.I. and MAS, R., 2006. Sedimentary evolution of the Torrecilla Reef Complex in response to tectonically forced regression (Early Kimmeridgian, Northern Spain). *Sedimentary Geology*, **183**, 31-49.

BEUTHER, A., 1966. Geologische Untersuchungen in Wealden und Utrillas-Schichten im Westteil der Sierra de los Cameros (Nordwestliche Iberische Ketten). *Beihefte zum Geologischen Jahrbuch* **44**, 103-121.

BORDENAVE, M.L., 1993. Applied petroleum geochemistry. Editions OPHRYS, 523 pp.

BÜKER, C., LITTKE, R. and WELTE, D.H., 1995. 2D-modelling of the thermal evolution of Carboniferous and Devonian sedimentary rocks of the eastern Ruhr basin and northern Rhenish Massif, Germany. *Zeitschrift der Deutschen Geologischen Gesellschaft,* **146**, 321-339.

CALLIES, M., DARNAULT, R., ANKA, Z., CORNU, T., LE GARZIC, E., WILLIEN, F. and GIBOREAU, R., 2018. New Tools for New Challenges: Petroleum System Modeling of the Kurdish Foothills. *AAPG Annual Convention & Exhibition 2018*. Salt Lake Ciy, USA.

CASAS, A.M., VILLALAÍN, J.J., SOTO, R., GIL-IMAZ, A., DEL RÍO, P. and FERNÁNDEZ, G., 2009. Multidisciplinary approach to an extensional syncline model for the Mesozoic Cameros Basin (N Spain). *Tectonophysics*, **470**, 3-20.

CASAS, A., RÍO, P., MATA, P., VILLALAÌN, J. and BARBERO, L., 2012. Comment on González-Acebrón *et al.* Criteria for the recognition of localization and timing of multiple events of hydrothermal alteration in sandstones illustrated by petrographic, fluid inclusion, and isotopic analysis of the Tera Group, Northern Spain. *International Journal of Earth Sciences*, **101**, 2043-2048.

CASAS, A. and SALAS, R., 1992. Historia de la subsistencia, anomalías gravimétricas y evolución mesozoica de las Cuencas del margen oriental de Iberia. *Actas de las sesiones científicas: III Congreso Geológico de España*, 112-116.

CASAS-SAINZ, A.M. and GIL-IMAZ, A., 1998. Extensional subsidence, contractional folding and thrust inversion of the eastern Cameros basin, northern Spain. *Geologische Rundschau*, **86**, 802-818.

CASQUET, C., GALINDO, C., GONZÁLEZ-CASADO, J. M., ALONSO, A., MAS, R., RODAS, M., GARCÍA, E. and BARRENECHEA, J.F., 1992. El metamorfismo en la Cuenca de los Cameros. Geocronología e implicaciones tectónicas. *Geogaceta*, **11**, 22-25.

CLEMENTE, P. and PÉREZ-ARLUCEA, M., 1989. Depositional architecture in fluviatile sediments. The pull-apart-type basin of Cameros (Spain) during the Lower Cretaceous extensional tectonic phase, *4th International Conference of Fluvial Sedimentology,* 103.

CORES, 2015a. Estadísticas Producción Interior de Crudo en el Mercado Español. *Corporación de Reservas Estratégicas de Productos Petrolíferos*. Madrid, 2.

CORES, 2015b. Estadísticas Producción Interior de Gas Natural en el Mercado Español. *Corporación de Reservas Estratégicas de Productos Petrolíferos*. 2.

DAVISON, I. and UNDERHILL, J.R., 2012. Tectonics and sedimentation in extensional rifts: Implications for petroleum systems. In: Gao, D. (Ed.), Tectonics and Sedimentation: Implications for Petroleum Systems. *AAPG Memoir*, **100**, 15-42.

DEL RÍO, P., BARBERO, L., MATA, P. and FANNING, C.M., 2009. Timing of diagenesis and very low-grade metamorphism in the eastern sector of the Sierra de Cameros (Iberian Range, Spain): a U-Pb SHRIMP study on monazite. *Terra Nova*, **21**, 438-445.

FERNÁNDEZ, M., MARZÁN, I., CORREIA, A. and RAMALHO, E., 1998. Heat flow, heat production, and lithospheric thermal regime in the Iberian Peninsula. *Tectonophysics*, **291**, 29-53.

GARCÍA, A. and MAS, R., 2004. Segunda fase de post-rifting:

Cretácico Superior. In: VERA, J.A. (Ed.), Geología de España. Sociedad Geológica de España; Instituto Geológico y Minero de España, Madrid, 510-522.

GONZÁLEZ-ACEBRÓN, L., GOLDSTEIN, R., MAS, R. and ARRIBAS, J., 2012. Answer to the comment of Casas *et al.* about González Acebrón *et al.*'s (2011) paper. *International Journal of Earth Sciences*, **101**, 1-5.

GONZÁLEZ-ACEBRÓN, L., GOLDSTEIN, R.H., MAS, R. and ARRIBAS, J., 2011. Criteria for recognition of localization and timing of multiple events of hydrothermal alteration in sandstones illustrated by petrographic, fluid inclusion, and isotopic analysis of the Tera Group, Northern Spain. *International Journal of Earth Sciences*, **100**, 1811-1826.

GUIMERÀ, J., ALONSO, Á. and MAS, J.R., 1995. Inversion of an extensional-ramp basin by a newly formed thrust: the Cameros Basin (N. Spain). In: BUCHANAN, J.G. and BUCHANAN, P.G. (Eds.), Basin Inversion. *Geol.Soc. Lond., Spec. Publ.*, **88**, 433-453.

GUIRAUD, M. and SÉGURET, M., 1985. A releasing solitary overstep model for the late Jurassic-early Cretaceous (Wealdian) Soria strike-slip basin (Northern Spain). In: BIDDLE, K.T. and CHRISTIE-BLICK, N. (Eds), Strike Slip Deformation, Basin Formation and Sedimentation. *Society of Economic Paleontologists and Mineralogists Special Publication*, **37**, 159-175.

HANTSCHEL, T. and KAUERAUF, A.I., 2009. Fundamentals of basin and petroleum systems modeling. Springer, Berlin, 475pp.

IES, 2007. PetroMod 2D Advanced, Tutorial Software Version 10. IES, GmbH Integrated Exploration System, Aachen, IES, GmbH Integrated Exploration System, Aachen, 139 pp.

LANAJA, J. M., 1987. Contribución de la exploración petrolífera al conocimiento de la geología de España. Instituto Geológico y Minero de España, Madrid, 465pp.

LEINFELDER, R. R., 1994. Distribution of Jurassic reef types: a mirror of structural and environmental changes during breakup of Pangea. In: EMBRY, A. F., BEAUCHAMP, B. and GLASS, D. J., Global environment and resources. *Memoirs of the Canadian Society of Petroleum Geologists*, **17**, 677-700.

LITTKE, R., U. BAYER, GAJEWSKI, D. and S. NELSKAMP, 2008. Dynamics of Complex Intracontinental Basins: The Central European Basin System. Springer, Berlin, 519pp.

MAGOON, L. B. and DOW, W. G., 1994. The petroleum system. In: MAGOON, L.B. and DOW, W. G., (Eds), The petroleum system -- from source to trap. *AAPG Memoir*, **60**, 3-24.

MANN, P., GAHAGAN, L. and GORDON, M. B., 2003. Tectonic setting of the world's giant oil and gas fields. In: HALBOUTY, M.T. (Ed.), Giant oil and gas fields of the decade 1990-1999. *AAPG Memoir*, **78**, 15-105.

MANTILLA-FIGUEROA, L. C., CASQUET, C. and MAS, J. R., 1998. Los paleofluidos en el Grupo Oncala, Cuenca de Cameros (la Rioja, España): Datos de inclusiones fluidas, isótopos de oxígeno y SEM. *Geogaceta*, **24**, 207-210.

MANTILLA-FIGUEROA, L.C., 1999. El metamorfismo hidrotermal de la Sierra de Cameros (La Rioja, España): petrología, geoquímica, geocronología y contexto estructural de los procesos de interacción fluido-roca. Doctoral Thesis, Universidad Complutense de Madrid, 361 pp.

MARTÍN-CLOSAS, C., 1989. Els caròfits del Cretaci inferior de les conques perifèriques del bloc de l'Ebre. Tesis, Universitat de Barcelona, 581 pp.

MARTÍN-CLOSAS, C. and ALONSO-MILLÁN, Á., 1998. Estratigrafía y bioestratigrafía (Charophyta) del Cretácico inferior en el sector occidental de la cuenca de Cameros (Cordillera Ibérica). *Revista de la Sociedad Geológica de España*, **11**, 253-269.

MARTÍNEZ DEL OLMO, W. and MALLO GARCÍA, J.M., 2002. Non-renewable energy resources: oil and gas. In: GIBBONS, W. and MORENO, T. (Eds), The Geology of Spain. Geological Society of London, 494-499.

MAS, R., ALONSO, Á. and GUIMERÀ, J., 1993. Evolución tectonosedimentaria de una cuenca extensional intraplaca: La cuenca finijurásica-eocretácica de Los Cameros (La Rioja-Soria). *Revista de la Sociedad Geológica de España*, **6**, 129-144.

MAS, R., GARCÍA, A., SALAS, R., MELÉNDEZ, A., ALONSO, A., AURELL, M., BÁDENAS, B., BENITO, M.I., CARENAS, B., GARCÍA-HIDALGO, J.F., GIL, J., SEGURA, M. , 2004. Segunda fase de rifting: Jurásico Superior-Cretácico Inferior. In: Vera, J.A. (Ed), Geología de España. SGE-IGME, SGE-IGME, 503-510.

MAS, R., BENITO, M. I., ARRIBAS, J., ALONSO, A., ARRIBAS, M.E., GONZÁLEZ-ACEBRÓN, L., HERNÁN, J., QUIJADA, E., SUÁREZ, P. and OMODEO-SALÉ, S., 2011. Evolution of an intra-plate rift basin: the Latest Jurassic-Early Cretaceous Cameros Basin (Northwest Iberian Ranges, North Spain). In: Sociedad Geológica de España, *Post-Meeting field trips 28th IAS Meeting*, Zaragoza (Spain), 117-154.

MAS, R., BENITO, M. I., ARRIBAS, J., SERRANO, A., GUIMERÀ, J., ALONSO, Á. and ALONSO-AZCÁRATE, J., 2002. La Cuenca de Cameros: desde la extensión finijurásica-eocretácica a la inversión Terciaria - Implicaciones en la exploración de hidrocarburos. *Zubía Monográfico*, **14**, 9-64.

MAS, R., M. I. BENITO, J. ARRIBAS, A. SERRANO, J. GUIMERÀ, Á. ALONSO, and J. ALONSO-AZCÁRATE, 2003. Geological Field Trip 11: The Cameros Basin: From Late Jurassic-Early Cretaceous Extension to Tertiary Contractional Inversion - Implications of Hydrocarbon Exploration. AAPG International Conference and Exhibition. Barcelona, 1-52.

MAS, R., ARRIBAS, M.E., GONZÁLEZ-ACEBRÓN, L., QUIJADA, I.E., CAMPOS-SOTO, S., SUAREZ-GONZALEZ, P., SACRISTÁN-HORCAJADA, S., ARRIBAS, J., BENITO, M.I. and PÉREZ-GARRIDO, C., 2018. Coastal wetlands as markers of transgression in proximal extensional systems (Berriasian, W Cameros Basin, Spain). *Journal of Iberian Geology,* 1-27.

MATA, M. P., CASAS, A. M., CANALS, A., GIL, A. and POCOVÍ, A., 2001. Thermal history during Mesozoic extension and Tertiary uplift in the Cameros Basin, northern Spain. *Basin Research*, **13**, 91-111.

McKENZIE, D., 1978. Some remarks on the development of sedimentary basins. *Earth and Planetary Science Letters*, **40**, 25-32.

MUÑOZ-JIMÉNEZ, A. and CASAS-SAINZ, A. M., 1997. The Rioja Trough (N Spain): tectosedimentary evolution of a symmetric foreland basin. *Basin Research*, **9**, 65-85.

OCHOA, M., ARRIBAS, J., MAS, R. and GOLDSTEIN, R. H., 2007. Destruction of a fluvial reservoir by hydrothermal activity (Cameros Basin, Spain). *Sedimentary Geology*, **202**, 158-173.

OMODEO-SALÉ, S., 2014. Thermal and sedimentary modelling of an intraplate extensional basin (Cameros Basin, North of Spain): Application for a hydrocarbon prospecting, Doctoral Thesis, Universidad Complutense de Madrid, 481 pp.

OMODEO-SALÉ, S., GUIMERÀ, J., MAS, R. and ARRIBAS, J., 2014. Tectono-stratigraphic evolution of an inverted extensional basin: the Cameros Basin (north of Spain). *International Journal of Earth Sciences*, **103**, 1597-1620.

OMODEO-SALÉ, S., I. SUÁREZ-RUIZ, J. ARRIBAS, R. MAS, L. MARTÍNEZ, and M. J. HERRERO, 2016. Characterization of the source rocks of a paleo-petroleum system (Cameros Basin) based on organic matter petrology and geochemical analyses. *Marine and Petroleum Geology*, **71**, 271-287.

OMODEO-SALÉ, S., SALAS, R., GUIMERÀ, J., ONDRAK, R., MAS, R., ARRIBAS, J., SUÁREZ-RUIZ, I. and MARTINEZ, L., 2017. Subsidence and thermal history of an inverted Late Jurassic-Early Cretaceous extensional basin (Cameros, North-central Spain) affected by very low- to low-grade metamorphism. *Basin Research*, **29**, 156-174.

OMODEO-SALÉ, S. and SUÁREZ-RUIZ, I., 2017. Spent hydrocarbon systems: a study case. In: SUÁREZ-RUIZ, I. and MENDONÇA-FILHO, J.G. (Eds), The role of organic petrology in the exploration of conventional and unconventional hydrocarbon system. *Geology: Current and future developments,* **1**, 287-320.

PALACIOS, P., 1890. Descripción fisica, geológica y agrológica de la provincia de Soria. In: TELLO, M. (Ed.), Memoria de la Comisión del Mapa Geologíco de España, 558.

PEPPER, A. S. and CORVI, P. J., 1995. Simple kinetic models of petroleum formation. Part I: oil and gas generation from kerogen. *Marine and Petroleum Geology*, **12**, 291-319.

PERMANYER, A., SALAS, R., MAS, R. and ARRIBAS, J., 2011. Geochemical characterization of tar sands in southern Cameros Basin: implications for source rocks derivation. 28th *International Association of Sedimentologists Meeting of Sedimentology*, 572.

PERMANYER, A., MÁRQUEZ, G. and GALLEGO, J. R., 2013. Compositional variability in oils and formation waters from the Ayoluengo and Hontomín fields (Burgos, Spain). Implications for assessing biodegradation and reservoir compartmentalization. *Organic geochemistry*, **54**, 125-139.

POELCHAU, H., BAKER, D., HANTSCHEL, T., HORSFIELD, B. and WYGRALA, B., 1997. Basin simulation and the design of the conceptual basin model, Petroleum and basin evolution. In: WELTE, D.H., HORSFIELD, B. and BAKER, D. R. (Eds), Petroleum and basin evolution: insights from petroleum geochemistry, geology and basin modelling, Springer, Berlin, 3-70.

PROYECTO VIURA, 2014. UNION FENOSA GAS, S.A. Oil & Gas Skills – OGS; Hidrocarburos de Euskadi – SHESA. FuturENERGY.

PUCHE, O., 2015. Algunos datos para la historia de la minería den la provincia de Soria. *Revista de Soria*, **90**, 3-26.

QUESADA, S., DORRONSORO, C., ROBLES, S., CHALER, R. and GRIMALT, J.O., 1997. Geochemical correlation of oil from the Ayoluengo field to Liassic black shale units in the southwestern Basque-Cantabrian Basin (northern Spain). *Organic Geochemistry*, **27**, 25-40.

QUIJADA, I. E., SUÁREZ GONZÁLEZ, P., MORENO, B., ISABEL, M. and MAS, J., 2013. New insights on stratigraphy and sedimentology of the Oncala Group (eastern Cameros Basin): implications for the paleogeographic reconstruction of NE Iberia at Berriasian times. *Journal of Iberian Geology*, **39**, 313-334.

QUIJADA, I. E., SUAREZ-GONZALEZ, P., BENITO, M.I. and MAS, R., 2013. Depositional Depth of Laminated Carbonate Deposits: Insights From the Lower Cretaceous Valdeprado Formation (Cameros Basin, Northern Spain). *Journal of Sedimentary Research*, **83,** 241-257.

QUIJADA, I.E., SUAREZ-GONZALEZ, P., BENITO, M.I. and MAS, R., 2016. Tidal versus continental sandy-muddy flat deposits: evidence from the Oncala Group (Early Cretaceous, N Spain). Contributions to modern and ancient tidal sedimentology: Proceedings of the Tidalites 2012 conference. John Wiley & Sons, 133-159.

RAHIMI, P., GENTZIS, T., DAWSON, W. H., FAIRBRIDGE, C., KHULBE, C., CHUNG, K., NOWLAN, V. and DEL BIANCO, A., 1998. Investigation of coking propensity of narrow cut fractions from Athabasca bitumen using hot-stage microscopy. *Energy & Fuels*, **12**, 1020-1030.

ROYDEN, L., 1986. A simple method for analyzing subsidence and heat flow in extensional basins. In: BURRUS, J. (Ed.), Thermal Modeling in Sedimentary Basins. Ed. Technip, Paris, **44**, 49-73.

ROYDEN, L. and KEEN, C., 1980. Rifting process and thermal evolution of the continental margin of eastern Canada determined from subsidence curves. *Earth and Planetary Science Letters*, **51,** 343-361.

SALAS, R. and CASAS, A., 1993. Mesozoic extensional tectonics, stratigraphy and crustal evolution during the Alpine cycle of the eastern Iberian basin. *Tectonophysics*, **228**, 33-55.

SALAS, R., GUIMERÀ, J., MAS, R., MARTÍN-CLOSAS, C., MELÉNDEZ, A. and ALONSO, Á., 2001. Evolution of the Mesozoic Central Iberian Rift System and its Cainozoic inversion (Iberian chain). In: ZIEGLER, P.A., CAVAZZA, W. F., and CRASQUIN-SOLEAU, S. (Eds.), Peri-Tethys Memoir 6: Peri-Tethyan Rift/Wrench Basins and Passive Margins. *Mémoires du Museum National d'Histoire Naturelle*, **186**, 145-186.

SALOMON, J., 1982a. Les formations continentales du bassin de Soria (Sierra de los Cameros) au Cretace inferieur: relation entre tectonique et sedimentation, Segundo Coloquio de Estratigrafía y Paleogeografía del Cretácico de España. Grupo Espanol del Mesozoico, 14.

SALOMON, J., 1982b. Les formations continentales du Jurassique Supérieur-Crétacé Inférieur (Espagne du Nord-Chaînes Cantabrique et NW Ibérique): stratigraphie, sédimentologie, cartographie, relations entre tectonique et sédimentation, *Mémoires Géologiques de l'Université de Dijon*. Institut des Sciences de la Terre, **6**, 228pp.

SALOMON, J., 1983. Le Crétacé inférieur continental. Le Fosse de Soria, Vue Sur le Crétacé Basco-Cantabrique et Nord-Ibérique. *Mémoires Géologiques de l'Université de Dijon*. Institut des Sciences de la Terre, **9**, 25-43.

SANZ, R., 1967. Ayoluengo Field. Southwest Cantabrian Basin North-Central Spain. *7th World Petroleum Congress*.

SCHUDACK, M., 1987. Charophytenflora und fazielle Entwicklung der Grenzschichten mariner Jura/Wealden in den Nordwestlichen Iberischen Ketten (mit Vergleichen zu Asturien und Kantabrien). *Palaeontographica Beiträge zur Naturgeschichte der Vorzeit, Abteilung B*, **204**, 1-180.

SECRETARÍA DE ESTADO DE ENERGÍA, 2014. Mapa de posición de Permisos de Investigación y concesiones de Explotación y Almacenamiento Subterráneo. Ministerio de Industria, Energía y Turismo. Gobierno de España, 15.

SUÁREZ GONZÁLEZ, P., QUIJADA, I.E., MAS, J. and BENITO, M.I., 2010. Nuevas aportaciones sobre la influencia marina y la edad de los carbonatos de la Fm Leza en el sector de Préjano (SE de La Rioja). Cretácico Inferior, Cuenca de Cameros. *Geogaceta*, **49**, 7-10.

SUÁREZ-GONZÁLEZ, P., QUIJADA, I.E., BENITO, M.I. and MAS, R., 2013. Eustatic versus tectonic control in an intraplate rift basin (Leza Fm, Cameros Basin). Chronostratigraphic and paleogeographic implications for the Aptian of Iberia. *Journal of Iberian Geology*, **39**, 285-312.

SUÁREZ-GONZÁLEZ, P., QUIJADA, I.E., BENITO, M.I. and MAS, R., 2015. Sedimentology of ancient coastal wetlands: insights from a Cretaceous multifaceted depositional system. *Journal of Sedimentary Research*, **85**, 95-117.

SUÁREZ-RUIZ, I., FLORES, D., MENDONÇA FILHO, J.G. and HACKLEY, P.C., 2012. Review and update of the applications of organic petrology: Part 1, geological applications. *International Journal of Coal Geology,* **99**, 54-112.

SWEENEY, J. J. and BURNHAM, A. K., 1990. Evaluation of a Simple Model of Vitrinite Reflectance Based on Chemical Kinetics. *AAPG Bulletin*, **74**, 1559-1570.

TAYLOR, G., TEICHMÜLER, M., DAVIS, A., DIESSEL, C., LITTKE, R. and ROBERT, P., 1998. Organic petrology. Gebrüder Borntraeger, Stuttgart, 704 pp.

TEICHMULLER, M., 1973. Generation of petroleum-like substances in coal seams as seen under the microscope. *Advances in organic geochemistry, 1973*, 321-348.

TEICHMÜLLER, M., 1974. Entstehung und Veränderung bituminöser Substanzen in Kohlen in Beziehung zur Entstehung und Umwandlung des Erdöls. *Fortschr. Geol. Rheinl. Westfalen*, **24**, 65-112.

TISCHER, G., 1965. Über die Wealden-Ablagerung und die Tektonik der östlichen Sierra de los Cameros in den nordwestlichen Iberischen Ketten (Spanien). *Beihefte zum*

Geologischen Jahrbuch, **44**, 123-164.
TISCHER, G., 1966. El delta weáldico de las Montañas Ibéricas Occidentales y sus enlaces tectónicos. *Notas y Comunicaciones del Instituto Geológico y Minero de España*, **81**, 53-78.
TISSOT, B., PELET, R. and UNGERER, P., 1987. Thermal history of sedimentary basins, maturation indices, and kinetics of oil and gas generation. *AAPG Bulletin*, **71**, 1445-1466.
UNGERER, P., BURRUS, J., DOLIGEZ, B., CHENET, P. and BESSIS, F., 1990. Basin Evaluation by Integrated Two-Dimensional Modeling of Heat Transfer, Fluid Flow, Hydrocarbon Generation, and Migration. *AAPG Bulletin*, **74**, 309-335.
VERA, J.-A., 2001. Evolution of the South Iberian continental margin. *Mémoires du Muséum national d'histoire naturelle*, **186**, 109-143.
VERGES, J. and GARCIA-SENZ, J., 2001. Mesozoic evolution and Cainozoic inversion of the Pyrenean rift. *Mémoires du Muséum national d'histoire naturelle*, **186**, 187-212.
WELTE, D. and YUKLER, M., 1981. Petroleum origin and accumulation in basin evolution – a quantitative model. *AAPG Bulletin*, **65**, 1387-1396.
WELTE, D. H., HORSFIELD, B. and BAKER, D. R., 1997. Petroleum and basin evolution: insights from petroleum geochemistry, geology and basin modeling. Springer, Berlin, 534 pp.
WYGRALA, B., 1989. Integrated study of an oil field in the southern Po basin, northern Italy. Unpubl. doctoral thesis, Univ. Köln, *Berichte Kernforschungsanlage Jülich*, **2313**, 217
YALÇIN, M., LITTKE, R. and SACHSENHOFER, R., 1997. Thermal history of sedimentary basins, Petroleum and basin evolution. In: WELTE, D.H., HORSFIELD, B. and BAKER, D.R. (Eds.), Petroleum and basin evolution: insights from petroleum geochemistry, geology and basin modelling, Springer, Berlin, 71-167.

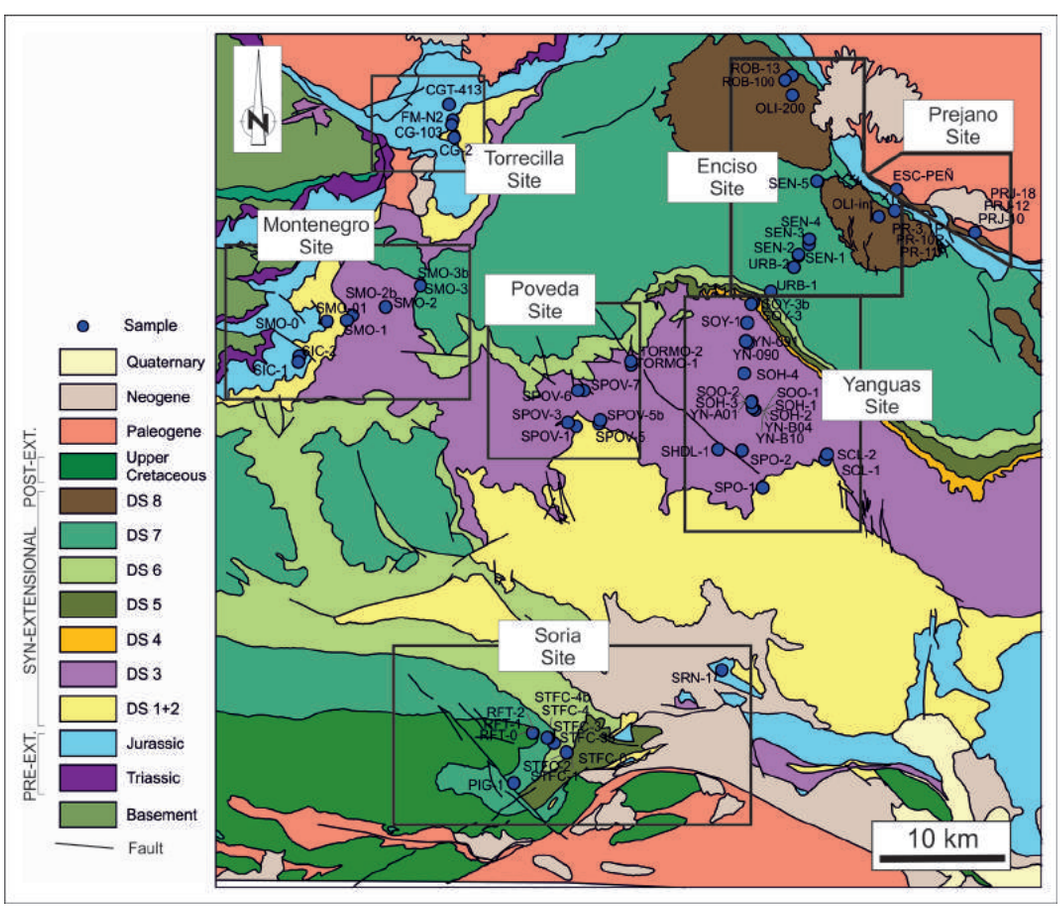

Appendix 1. Location of the samples analysed for vitrinite reflectance and Rock-Eval measurements whose results are shown in Fig. 5.

Site	Unit	ID-Sample	TOC [%]	PC [%]	RC [%]	HI [mg HC/g TOC]	OI [mg CO2/g TOC]	Tmax [°C]*	S1 [mg HC/g]	S2 [mg HC/g]	S3
Torrecilla	Marine Jurassic - Torrecilla Fm	FM-N2	0.24	0.03	0.22	44	238	450	0.03	0.11	0.58
		CGT-413	0.19	0.02	0.16	52	223	423	0.05	0.10	0.42
		CG-103	0.12	0.02	0.10	63	400	426	0.01	0.08	0.48
		CG-2	0.20	0.03	0.17	60	281	293	0.05	0.12	0.55
Montenegro	DS3 Huerteles Fm	SMO-3b	1.83	0.02	1.81	4	29	303	0.03	0.08	0.54
		SMO-3	1.77	0.02	1.75	3	28	-	0.02	0.05	0.50
		SMO-2	0.41	0.01	0.40	5	62	-	0.01	0.02	0.25
		SMO-2b	0.24	0.02	0.22	27	200	494	0.02	0.07	0.48
	DS1+2 Magaña Fm	SMO-1	0.20	0.02	0.18	20	117	-	0.09	0.04	0.23
		SMO-01	1.91	0.00	1.91	2	4	-	0.02	0.04	0.08
	Marine Jurassic - Torrecilla Fm	SMO-0	0.28	0.02	0.27	23	101	441	0.02	0.07	0.29
	Marine Jurassic - Pozalmuro Fm	SIC-2	0.68	0.02	0.65	10	52	381	0.11	0.07	0.35
		SIC-1	0.75	0.03	0.73	9	55	375	0.10	0.07	0.41
Poveda	DS3 - Huerteles Fm	TORMO-2	0.91	0.00	0.91	0	7	-	0.01	0.00	0.06
		TORMO-1	1.18	0.01	1.17	3	38	-	0.02	0.03	0.45
		SPOV-7	0.47	0.02	0.45	16	74	495	0.03	0.08	0.35
		SPOV-6	0.10	0.02	0.08	101	179	390	0.02	0.10	0.17
		SPOV-5b	0.09	0.02	0.07	51	411	-	0.02	0.04	0.35
		SPOV-5	0.13	0.03	0.10	114	219	496	0.02	0.14	0.27
	DS1+2 - Magaña Fm	SPOV-4	0.33	0.01	0.31	27	56	495	0.02	0.09	0.18
		SPOV-3	0.47	0.04	0.43	26	203	439	0.01	0.12	0.95
		SPOV-2	0.43	0.02	0.42	15	94	496	0.02	0.07	0.41
		SPOV-1	0.36	0.02	0.34	9	113	-	0.01	0.03	0.40
Enciso	DS8 - Oliván Gr	ROB-100	3.85	0.01	3.84	0	15	-	0.01	0.00	0.58
		ROB-13	1.33	0.01	1.32	0	24	-	0.01	0.00	0.32
		OLI-200	2.04	0.02	2.02	0	35	-	0.02	0.00	0.71
	DS7 - Leza Fm	PR-11P	0.11	0.01	0.10	0	394	-	0.01	0.00	0.44
		PR-10P	0.27	0.03	0.24	38	296	429	0.06	0.10	0.81
		PR-3.1P	0.17	0.01	0.16	0	237	-	0.00	0.00	0.41
		SOTO-02P	0.11	0.01	0.10	0	401	-	0.00	0.00	0.45
	DS7 - Enciso Gr	SEN-5	1.11	0.00	1.11	1	8	-	0.02	0.01	0.09
		SEN-4	1.50	0.03	1.47	6	60	495	0.02	0.09	0.90
		SEN-3	1.45	0.02	1.43	6	39	333	0.03	0.09	0.57
		SEN-2	1.68	0.02	1.66	4	21	367	0.03	0.06	0.36
		SEN-1	0.27	0.02	0.25	32	70	379	0.17	0.09	0.19
	DS7 - Urbión Gr	URB-2	0.13	0.01	0.12	57	207	347	0.02	0.07	0.27
		URB-1	1.34	0.02	1.32	4	44	-	0.03	0.05	0.59
Yanguas	DS3 - Valdeprado Fm	SOY-3b	0.37	0.01	0.36	21	17	345	0.02	0.08	0.06
		SOY-3	0.32	0.01	0.31	17	39	-	0.03	0.05	0.12
		SOY-1	0.50	0.02	0.48	0	119	-	0.02	0.00	0.59
		YN-091	0.57	0.02	0.55	0	132	-	0.00	0.00	0.74
		YN-090	3.81	0.12	3.69	26	27	434	0.11	0.97	1.02
		SOH-4	0.98	0.02	0.96	2	68	-	0.03	0.02	0.67
		YN-A01	0.48	0.03	0.45	13	147	495	0.02	0.06	0.71
		SOH-3	2.22	0.04	2.18	3	41	319	0.03	0.06	0.90
		SOO-2	0.86	0.02	0.84	6	56	-	0.07	0.05	0.48
		YN-B10	0.56	0.02	0.54	14	69	332	0.04	0.08	0.39
		YN-B08	0.28	0.04	0.24	24	412	358	0.03	0.07	1.15
		YN-B04	0.65	0.03	0.62	10	114	418	0.03	0.07	0.74
		SOH-2	2.31	0.04	2.27	4	37	313	0.05	0.10	0.86
		SOH-1b	0.60	0.02	0.58	13	80	433	0.02	0.08	0.48
		SOH-1	0.50	0.02	0.48	6	114	-	0.01	0.03	0.57
		SOO-1	0.18	0.02	0.16	43	136	365	0.13	0.08	0.25
	DS3- Huerteles	SPO-2	0.38	0.02	0.36	29	46	477	0.03	0.11	0.17
		SHDL-1	1.37	0.03	1.34	4	56	-	0.03	0.05	0.77
	DS1+2 - Matute Fm	SPO-1	0.27	0.02	0.25	16	185	-	0.01	0.04	0.50
		SCL-2	0.45	0.02	0.43	10	126	-	0.02	0.04	0.57
		SCL-1	0.20	0.02	0.18	32	228	-	0.02	0.06	0.46
Prejano	DS8 - Escucha Fm	PRJ 18	3.21	0.31	2.9	99	45	435	0.06	3.17	1.43
		PRJ 12	6.30	0.58	5.72	89	62	439	0.06	5.64	3.90
		PRJ 10	41.35	16.70	24.65	476	19	416	1.95	196.64	7.73
		ESC-PEÑ	15.09	1.08	14.01	71	43	423	0.18	10.69	6.54
Soria	DS7 - Abejar Fm	PIG-1	1.52	0.99	0.53	714	27	433	0.90	10.85	0.41
		STFC-4b	3.95	0.34	3.61	81	70	431	0.04	3.19	2.78
		STFC-4	3.48	0.11	3.37	28	28	427	0.04	0.99	0.96
		STFC-3b	2.84	0.08	2.76	10	73	431	0.05	0.27	2.07
		STFC-3	2.21	0.07	2.14	7	88	480	0.04	0.16	1.94
	DS6 - Pantano Fm	STFC-2	2.67	0.13	2.54	12	135	477	0.02	0.33	3.62
		STFC-1	5.44	0.16	5.28	12	73	434	0.03	0.63	3.97
		STFC-0	1.46	0.07	1.39	46	31	438	0.04	0.68	0.45
	Marine Jurassic - Pozalmuro Fm	SRN-1	0.17	0.01	0.15	33	174	-	0.02	0.05	0.29
Casarejos	DS7 - Abejar Fm	CAS-2	17.82	10.72	7.10	695	43	438	2.75	123.83	7.66

* Tmax is not considered in samples with S2 <0.05

Appendix 2. Rock-Eval data.

Site	Unit	ID-Sample	Type of particle	N. particles measured	%Ro_Mean	Deviation Standard
Torrecilla	Marine Jurassic - Torrecilla Fm	FM-N2	V	19	2.98	0.37
		CGT-413	V	16	2.5	0.37
		CG-103	V	13	3.3	0.40
		CG-2	V	20	3	0.20
Montenegro	DS3 - Huerteles Fm	SMO-3b	SB	16	3.9	0.87
		SMO-3	None	-	-	-
		SMO-2	V	10	3.8	0.57
		SMO-2b	Altered	-	-	-
	DS1+2 Magaña Fm	SMO-1	V	23	2.8	0.55
		SMO-01	V	12	3.34	0.23
	Marine Jurassic - Torrecilla Fm	SMO-0	V	6	4.45	0.44
	Marine Jurassic - Pozalmuro Fm	SIC-2	V	40	4.2	0.31
		SIC-1	V	21	4.2	0.75
Poveda	DS3 - Huerteles Fm	TORMO-2	V	20	4.6	0.47
		TORMO-1	V	5	3.7	0.46
		SPOV-7	V	21	3	0.43
		SPOV-6	None	-	-	-
		SPOV-5b	V	7	2.3	0.35
		SPOV-5	V	9	2.4	0.28
	DS1+2 - Magaña Fm	SPOV-4	Altered	-	-	-
		SPOV-3	V	17	2	0.55
		SPOV-2	V	18	2.3	0.51
		SPOV-1	V	18	2.2	0.51
Enciso	DS8 - Oliván Gr	ROB-100	V	50	3.2	0.13
		ROB-13	V	50	3	0.25
		OLI-200	V	16	2.86	0.25
	DS7 - Leza Fm	PR-11P	SB	21	4.35	0.81
		PR-10P	None	-	-	-
		PR-3.1P	None	-	-	-
	DS7 - Enciso Gr	SOTO-02P	None	-	-	-
		SEN-5	V	22	2.4	0.87
		SEN-4	None	-	-	-
		SEN-3	V	22	3.88	0.79
		SEN-2	None	-	-	-
		SEN-1	V	4	2.09*	0.23
	DS7 - Urbión Gr	URB-2	V	18	3.2	0.52
		URB-1	None	-	-	-
Yanguas	DS3 - Valdeprado Fm	SOY-3b	V	20	2.9	0.88
		SOY-3	V	53	3	0.87
		YN-091	None	-	-	-
		YN-090	None	-	-	-
		SOY-1	None	-	-	-
		SOH-4	V	12	2.7	0.31
		YN-A01	None	-	-	-
		SOH-3	V	32	2.2	0.41
		SOO-2	V	27	2	0.23
		YN-B10	V	8	1.57	0.17
		YN-B08	None	-	-	-
		YN-B04	V	40	2.4	0.44
		SOH-2	V	20	2.05	0.26
		SOH-1b	V	10	1.9	0.19
		SOH-1	V	16	2.1	0.28
		SOO-1	V	23	1.9	0.42
	DS3- Huerteles	SPO-2	V	46	4.6	0.52
		SHDL-1	V	35	2.9	0.27
	DS1+2 - Matute Fm	SPO-1	V	3	3.5*	0.30
		SCL-1	V	27	3.1	0.63
		SCL-2	V	2	2.18*	0.02
Prejano	DS8 - Escucha Fm	ESC-PEÑ	V	35	0.62	0.08
		PRJ 18	V	50	0.63	0.04
		PRJ 12	None	-	-	-
		PRJ 10	V	80	0.56	0.11
Soria	DS7 - Abejar Fm	PIG-1	V	46	0.47	0.22
		STFC-4b	V	41	0.38	0.12
		STFC-4	V	31	0.5	0.21
		STFC-3b	Altered	-	-	-
		STFC-3	Altered	-	-	-
	DS6 - Pantano Fm	STFC-2	Altered	-	-	-
		STFC-1	V	58	0.57	0.17
		STFC-0	V	57	0.55	0.21
	Marine Jurassic - Pozalmuro Fm	SRN-1	None	-	-	-
Casarejos	DS7 - Abejar Fm	CAS-2	V	22	0.3	0.04

Appendix 3. Vitrinite reflectance data. Reflectance was measured mostly on vitrinite particles (V) and in a few cases on solid bitumen particles (SB).